STRUCTURAL BEHAVIOR OF DOUBLY CURVED SHELL STRUCTURE CONSTRUCTED WITH MUD-CONCRETE

Rohantha Rukshan Jayasinghe

198135N

Thesis submitted in partial fulfillment of the requirements for the degree Master of Science

Department of Civil Engineering

University of Moratuwa
Sri Lanka

February 2022

DECLARATION

I declare that this is my own work and this thesis does not incorporate without acknowledgement any material previously submitted for a degree or Diploma in any other University or institute of higher learning and to the best of my knowledge and belief it does not contain any material previously published or written by another person except where the acknowledgement is made in the text.

Also, I hereby grant to University of Moratuwa the non-exclusive right to reproduce and distribute my thesis/dissertation, in whole or in part in print, electronic or other medium. I retain the right to use this content in whole or part in future works (such as articles or books).

Signature: Date:

The above candidate has carried out research for the Masters under my supervision.

Name of the Supervisor: Prof. R.U.Halwatura

Signature of the supervisor: Date:

Name of the Supervisor: Eng. K.I.U.Nanayakkara

Signature of the supervisor: Date: UOM Verified Signature

Name of the Supervisor: Dr. Rizna Arooz

Signature of the supervisor: UOM Verified Signature Date: 22/02/2022

Abstract

Embodied carbon emissions have been overlooked in the past few decades. As such, today, the building sector is responsible for 38% of all carbon emissions in the world greenhouse gas emissions. To overcome the climate crisis, sustainable construction practices, reducing reliance on carbon insensitive raw materials usage and net-zero carbon standards are being implemented across the globe. Building with earthen materials becomes a focal point in sustainable building design practices since its an environmentally friendly construction practice. Although there are several earth-based modern construction techniques for walling available in Sri Lanka (such as rammed earth, mud-concrete), no reliable technique is developed or adopted as a slab system. Most of the recent earthen constructions are either single-storied or use concrete as their slab system. Thus, the earthen slab system would be a huge step towards a structure entirely made of earthen materials.

Here, it is attempted to identify the structural behavior of the doubly curved shell structure using Finite Element Analysis (FEA) and the possibility of constructing an earthen slab system using Mud-concrete. It was identified that nearly 50% of cost reduction can be expected when compared with the reinforced concrete slab systems. A 1m x1m prototype Mud-concrete slab was constructed to check the potential for modular construction practice with a square footprint. The masonry mould method was used as the formwork system by considering the ease of the construction. Shell thickness of 50mm is the primary structural component, while the non-structural filling of 50mm from apex was used with the Mud-concrete mixture used as a flat floor surface.

Key words: Doubly curved shells, Mud-concrete, Sustainable, Vault structures

DEDICATION

This dissertation is dedicated to my loving parents.

For their endless love, support and encouragement

ACKNOWLEDGEMENTS

My work towards a Master of Science Degree and this thesis would not have been successful if not for the guidance and support from many individuals who devoted their time and resources towards the success of this project.

I am very much thankful to my research supervisors, Prof. Rangika Halwatura, Eng. Isuru Nanayakkara and Dr. Rizna Arooz for their continues guidance and support throughout the research project. If not for their guidance and motivations this research project would not have gotten so far.

The research work included an extensive literature survey and study of historical earthen structures. I owe much to the long list of researchers who shared their work in various ways, including on ResearchGate® platform. The assistance provided by Dr. Will Hawkins in sharing his research results and providing clarifications is specially appreciated.

Prof. Kumari Gamage and Dr. Kasun Nandapala of the progress review committee and the fellow research assistants at Pro-Green Laboratory, Department of Civil Engineering of University of Moratuwa are acknowledged for their critical comments which were useful in refining and guiding the work towards a successful outcome.

The research work was partially funded by a short-term grant (SRC/ST/2020/21) from the Senate Research Committee of the University of Moratuwa.

Finally, I owe a huge debt of gratitude to my parents for believing in my work and supporting me in various ways, including financial assistance when needed.

TABLE OF CONTENT

LIST OF FIGURES

LIST OF TABLES

LIST OF ABBREVIATIONS

Abbreviations	**Description**
AD	Anno Domini
BC	Before Christ
FEA	Finite Element Analysis
FEM	Finite Element Method
LC	Load Case
MC	Mud Concrete
TNA	Thrust Network Analysis
TRC	Textile Reinforced Concrete
SDG	Sustainable Development Goals

LIST OF APPENDICES

1 INTRODUCTION

Building industry is one of the most significant contributors to environmental pollution as well as the largest user of materials and energy. Specially, considering the global carbon emission of the concrete and steel in building construction is about 8% and 9% respectively (IEA, 2008; Preston and Lehne, 2018). Altogether, concrete and steel production process cause about one-third of industrial carbon emission globally (Allwood et al., 2010). In response to these issues, sustainable practices and proper strategies and actions need to be adopted in the current building construction practices. For an ideal sustainable construction, it should need to be design with reusable materials or efficient resources, to reduce the CO_2 emission and it should harmonize with the nature. Moreover, it should be inexpensive and should require low maintenance cost during its lifespan.

Building with earthen materials are found to be the most sustainable solution to address the current situation. Although, new technologies and practices are employed to build sustainable constructions with earthen materials, most constructions are restricted to single storey buildings or use traditional reinforced concrete slab system for the design. Steel reinforcements are mainly used in the slab system to resist the tensile stresses. Since the tensile strength of the earthen materials are comparatively low, use of reinforcement with earthen materials is not suitable due to the corrosion.

As a solution to the issue, slab system with arching effect (compression-only form) would be a significant, which can be implemented a slab system using an earthen material.

1.1 Aims and objectives

This study aims to investigate the possibility of constructing a slab system using earthen materials. The main objectives of the research are;

i. To identify most suitable shell geometry for doubly curved shell structure
ii. To investigate the viability of mud concrete in vault construction
iii. To compare structural, environmental, and economic performance of shell structure using Mud-Concrete

1.2 Dissertation structure

Chapter 1 has introduced the motivation, aims and objectives of this research.

Chapter 2 reviews the relevant literature including impact of the construction sector, earthen construction, shell structures, analyzing methods for shells and suitable materials for the constructions.

Chapter 3 includes detailed assessment the proposed structural form, structural analysis including finite element modeling, construction, and load testing for material and for the physical model.

Chapter 4 provides the environmental and economic performance comparison of the proposed slab system with traditional reinforced concrete slab system and same structural form with concrete as a filling.

Chapter 5 provides broad conclusions and recommendations for the future works.

2 LITERATURE REVIEW

2.1 Impact of the construction sector to the climate change

Climate change and global warming are considered the most significant global challenges and environmental concerns in society nowadays. According to the National Oceanic and Atmospheric Administration (NOAA) of USA, since 1970's, carbon emissions have increased by about 90% (Menne et al., 2018).

Based on the global emission data, construction sector becomes the most significant sector that causes significant environmental impact by emitting a large amount of emission into the atmosphere (Guggemos and Horvath, 2006). In addition, the construction industry is considered the primary contributor to the environmental polluter of 40% of global use (Akadiri et al., 2012).

According to the Sustainable Development Goals (SDG 11-Sustainable cities and communities, SDG 12-Responsible consumption and production, SDG 13- Climate action), by 2050, two-thirds of the global population will be urban and sustainable development cannot be achieved without significantly changing or improving the current methods of construction or technologies ("Sustainable Development Goals (SDGs) and Disability," 2020). Therefore, a sustainable building design approach is considered a way for the construction industry to move towards by focusing on low-cost constructions and reducing material usage with efficient designs to respond to climate emergencies.

2.2 Earthen constructions as a sustainable design

As the global population increased, the use of world natural resources been depleted exponentially. Moreover, among the generated construction and demolition waste, 10-30% are dumped into landfills globally, causing environmental and socio-economic problems(Menegaki and Damigos, 2018).

To address the current crisis in the construction industry, sustainable materials were used as construction materials (e.g., Bamboo, wood, soil etc.). Lynn Froeschle stated that there are several green building material selection criteria. (i) Resource efficiency- (Resource efficiency of the material can be utilized by considering the recycled content, renewability, manufacturing process, durability), (ii) Indoor Air Quality (IAQ)– (materials which emit few or no carcinogens) (Dick, 2019; Froeschle, 1999).

Earth, one of the oldest construction materials throughout history (dates back to the period of El-Obeid in Mesopotamia - 5000-4000 BC) (Pollock, 1999), can still be used as a green building material for the modern construction industry. However, the popularity of earthen construction practices was decreased due to industrialization in the 18th century (Patnaik, 2018). However, due to the rising demand for affordable, sustainable materials, various earthen construction technologies and practices were resurfaced in recent years and building with earth becomes a global trend in developed countries and developing countries.

2.3 Development in earthen materials

The techniques and construction methods for earthen construction vary with the cultural aspects and available resources and techniques. Figure 2-1 shows the distribution of earthen constructions in world. Throughout civilizations, the earth was formed as various building materials such as cobs, wattle and daub, adobe blocks, earth bricks. Many historical earthen constructions made from these technologies can still be seen worldwide. Few examples are (i)Vaults of Ramesseum granaries made of adobes in Egypt -built around 1300 BC (Figure 2-2), (ii) Ksar of Aït-Ben-Haddou made of clay bricks in Morocco- build around 1100 BC (Figure 2-4),(iii) Tabo Monastery made of adobes in Spiti valley, India – built in 996 AD (Figure 2-3).

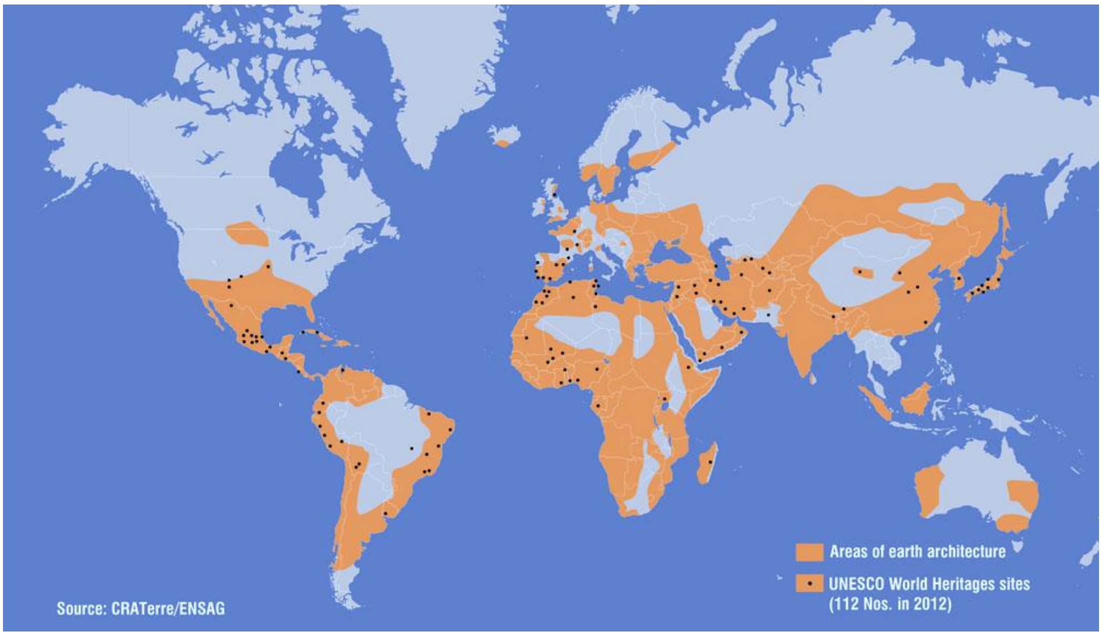

Figure 2-1: Distribution of earthen construction throughout the world
Source: Auroville Earth Institute


Figure 2-2: Vaults of Ramasseum, in Egypt- build in 1300 BC
Source: Auroville Earth Institute

Figure 2-4: Ksar of Aït-Ben-Haddou made of clay bricks in Morocco- build in 1100 BC
Source: archeyes.com

Figure 2-3: Tabo Monastery made of adobes in Spiti valley, India – built in 996 AD
Source: (Lee, 2013)

With the adaptation from these ancient earthen constructions, many researchers practice improved techniques such as Compressed Stabilized Earth Blocks (CSEB) rammed earth walls (Walker et al., 2005), mud concrete blocks and walls (Arooz and Halwatura, 2018), floor finishing systems (Galabada and Halwatura, 2019).

2.4 Challenges for modern earthen construction

Although many earthen construction techniques and practices are implemented for walling or flooring systems, most of the constructions are restricted to (i) either one or two storeys or (ii) use conventional slab systems for the design. When considered the conventional slab system or flooring system, most of the embodied energy in a typical multi-storey building structure (60% to 70%) exists within the floors (Foraboschi et al., 2014). As with population growth and urbanization, it is critical to find a better solution for modern earthen construction.

However, an ancient construction method of the “thin vaulting system” can still replace the roofing structures for single-storey buildings or dwelling units. Recent most popular projects that use vaulting technologies are (i) Central Market in Koudougou in Burkina Faso (Bolay, 2020) (Figure 2-5), (ii) SUDU housing prototype in Ethiopia (Block et al., 2010)(Figure 2-6), (iii) “Brick-o-Topia” (López et al., 2014) (Figure 2-7).

Figure 2-5: Central Market in Koudougou in Burkina Faso
Source: (Bolay, 2020)

Figure 2-6: SUDU housing prototype in Ethiopia
Source: (Block et al., 2010)

Figure 2-7: “Brick-o-Topia”, The Thin-Tile Vaulted Pavilion
source: (López et al., 2014)

2.5 Possibility of constructing a slab system using earthen materials

The strength of the earthen materials is comparatively low when compared with conventional concrete. Thus, it is not possible to create a typical flat slab system only by using earthen materials. Ockleston stated that “Restraining flat slabs laterally can increase their loading capacity by almost three times due to an arching effect known as compressive membrane action” (Ockleston, 1958). This increment is after steel has yielded and slab underside cracked. Since earthen materials has poor tensile capacity, it should start with the compressive membrane action. If an alternative slab system designed with the arching effect, it will behave under compressive loading and also it could significantly reduce the self-weight of the structure. The Figure 2-8 shows the structural efficiency increase through the arching effect.

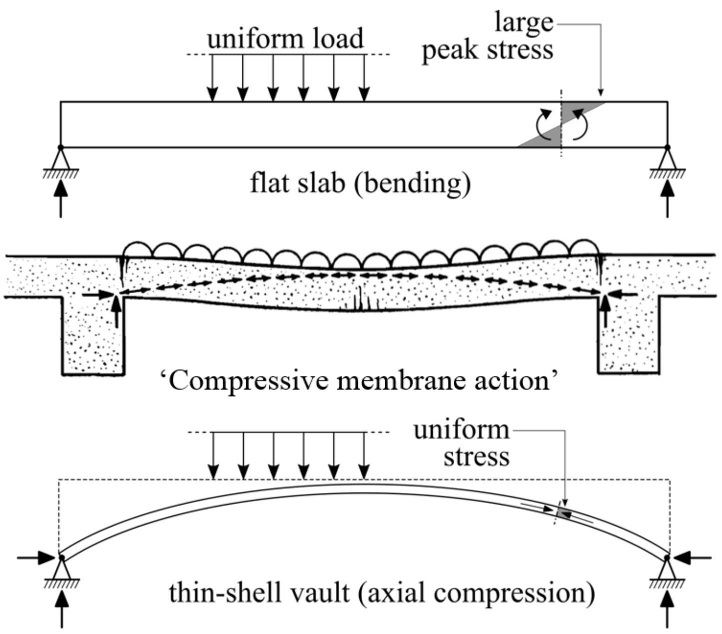

Figure 2-8: Structural efficiency increases through the arching effect
Source: (Hawkins et al., 2017)

Adaptation from the above construction practices, one of the possible earthen slab systems was identified as tile vault inspired earthen slab system (Jayasinghe et al., 2019), which uses thin tiles to build the shell while non-structural filling use as a ballast to see it as a floor (Figure 2-9).

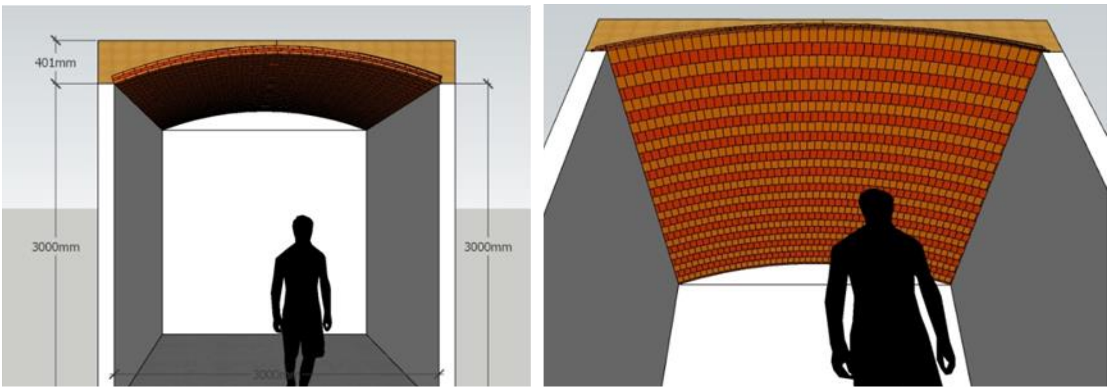

Figure 2-9: Catalan vault inspired earthen slab system
Source: (Jayasinghe et al., 2019)

2.6 Approach to shell structures

Shell structures are typically lightweight structures construct with shell elements. These shell structures gain their strength and rigidity with the curved forms. Typically, most thin shell structures are biomimicry structures inspired by nature. E.g., Sydney opera house in Australia – shape inspired from a peeled orange (Figure 2-10), Dalian shell museum in China – shape inspired from the seashell (Figure 2-11).

Figure 2-10: Sydney opera house in Australia
source: www.archdaily.com

Figure 2-11: Dalian shell museum in China
source: www.archdaily.com

2.6.1 Gaussian curvature of a shell structure

Gaussian curvature of a surface at a point (which denoted by ‘K’) is the product of the principal curvatures. The maximum and minimum of the normal curvature and at a given point on a surface are called the principal curvatures. Figure 2-12 shows the types of gaussian curvatures.

$$K = k_1 \times k_2 \quad (1)$$

Where;

k_1 and k_2 = Principal curvatures at a given point

a. If both principal curvatures are of the same sign, $k_1 \times k_2 > 0$, then the Gaussian curvature is positive and the surface can be identified as an ellipse.
b. If the principal curvatures have different signs, $k_1 \times k_2 < 0$, then the Gaussian curvature is negative, and the surface can be identified as hyperbolic
c. If one of the principal curvatures is zero, $k_1 \times k_2 = 0$, the Gaussian curvature is zero, and the surface can be identified as parabolic shape.

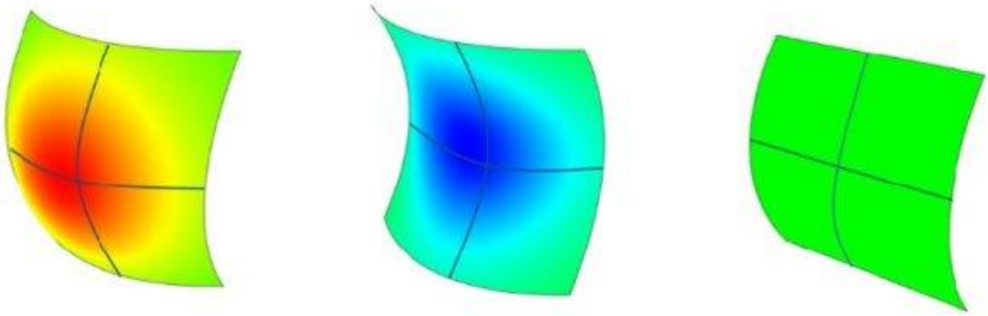

(a) (b) (c)

Figure 2-12: Types of gaussian curvatures
Source: (Neugebauer et al., 2018)

By considering the curvature, shells can be divided into singly curved shells (curvature on one linear axis with zero Gaussian curvature) and doubly-curved shells (curvature on both axes has positive Gaussian curvature). Doubly curved shells may have positive or negative Gaussian curvatures depending on the shape of the shell, which have non-developable surfaces. Thus, these doubly curved shells are more robust and stiffer and more stable than shells with zero Gaussian curvature (Michiels and Adriaenssens, 2017).

2.7 Form finding methods

Form finding method is a process that involves finding a structurally feasible shape. To build a compression-only form, the line of thrust should be within its middle third of the section and it is a stricter condition for no cracking scenario (line of thrust is an imaginary line representing the path of the resultant compressive forces). If the line of thrust lies within its cross-section, then the structure will be in compression. Nevertheless, if the thrust moves out of the cross section, tensile forces may form and cracks may develop in those areas. Further development of cracks may then results form of hinges and ultimately structure may collapse.

According to Heyman safe theorem, if any line of thrust lies within the middle third section, it will not collapse. Safety is a critical factor when designing any structure.

2.7.1 Line of thrust

A line of thrust is a theoretical line representing the path of the resultant of the compressive forces. It is essential to keep the thrust line within the cross-section (Figure 2-13) to prevent the formation of hinges and collapse due to tensions. For optimization, structures design to kept the line of thrust within its middle-third of the section as a safe condition for better stability.

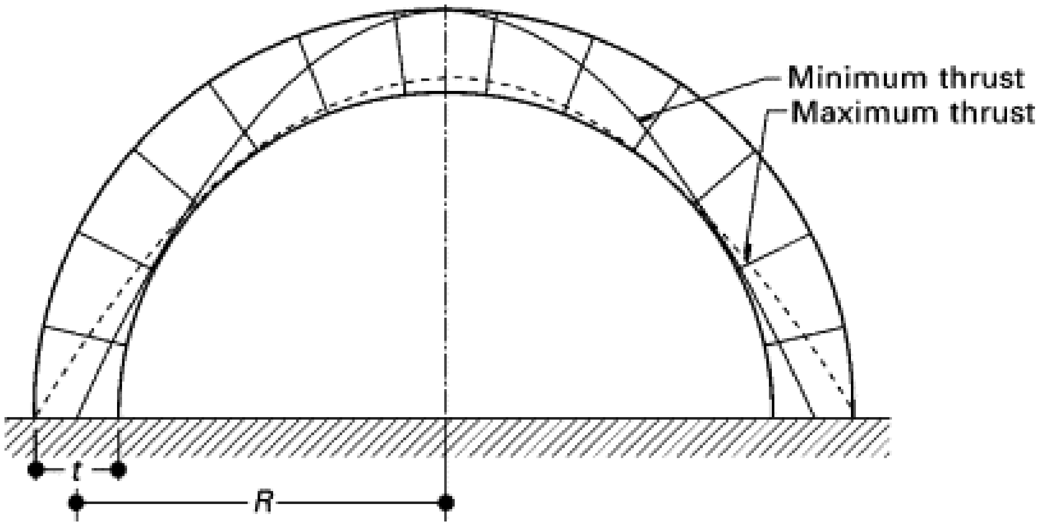

Figure 2-13: Minimum and maximum thrust in arch section
Source: (Dahmen & Ochsendorfs, 2012)

2.7.2 Hanging chain method

Robert Hooke (1675) was the first to propose that if a chain suspends freely from its ends, it will result in a hyperbolic cosine curve (also known as Catenary curve), and it will distribute the static load of the chain evenly between its links. When the shape of the chain inverted vertically, it gives a compression-only form resulting in an optimum arch shape. However, this method was well known for centuries specially in Greek and Roman arches, but Gaudí, effectively develops a parametric design process using this tension-compression scenario in a chain hanging method (Moriana, 2012).

Similarly, Heinz Isler also used a hanging cloth reversed method to finding suitable forms for his shells. The fabric surface is dipped into plaster and hung by its ends, and after its thoroughly dried, the inverted shape is a complete compression form (Figure 2-14 & Figure 2-15).

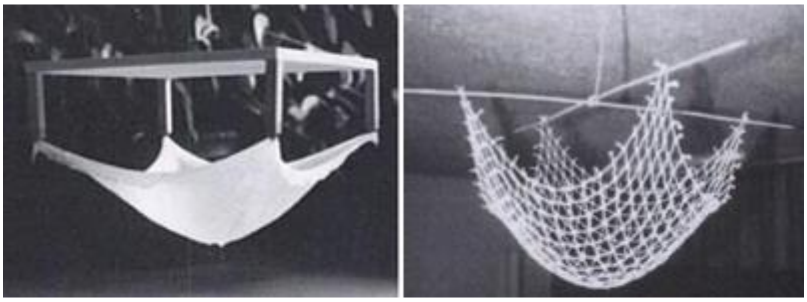

Figure 2-14: Heinz Isler's hanging cloths method
Source: (Isono, 2009)

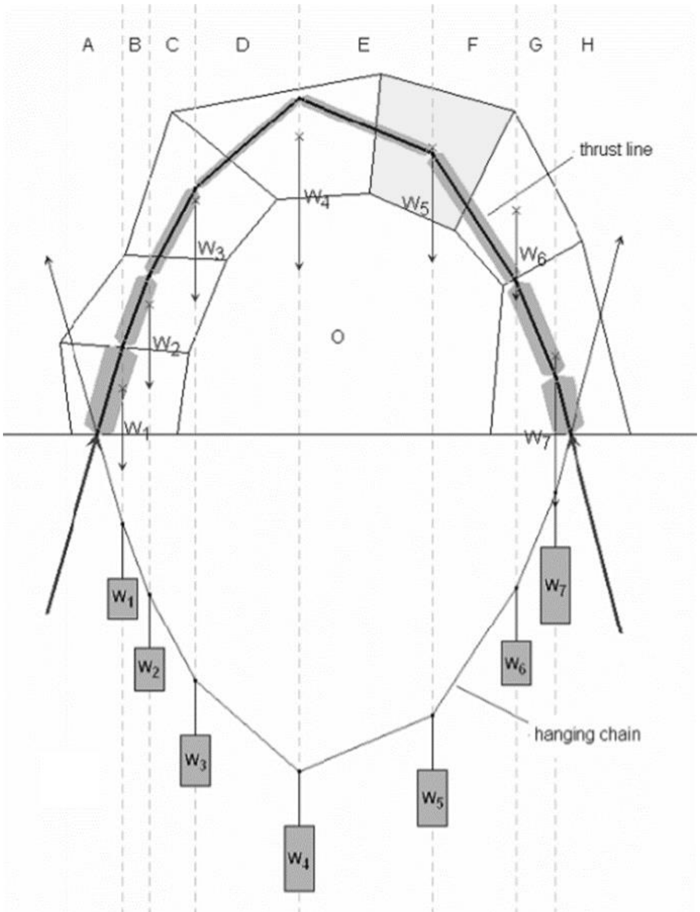

Figure 2-15: Hanging chain with weights applied to the chain and its inverted form and with thrust line through the curve
Source: (Block et.al.,2006)

2.7.3 Graphic Static Method

One of the easiest methods is to use a graphical representation of compressive forces acting on the structure to find the line of thrust. It can identify the best suitable shape of the arch and behavior and failure of the arch during different load cases. Developing a thrust line is based on the form of a line by connecting the centroid of each block. Using a funicular polygon diagram line of thrust can be found (Figure 2-16).

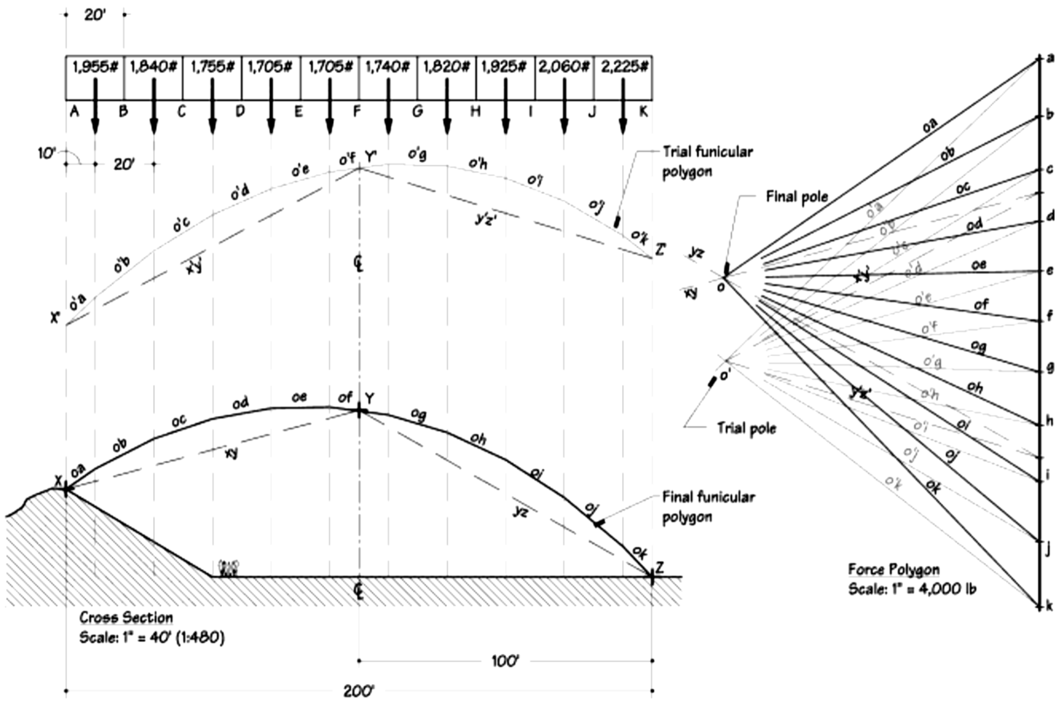

Figure 2-16: Graphic static method
Source: (Allen & Zalewski, 2010)

2.7.4 Finite Element Method (FEM)

Finite Element Method (FEM) is one of the most commonly used methods in structural analysis. It is a numerical technique that uses Finite Element Analysis (FEA) to determine the distribution of forces/ stresses, displacements/ strains in a structure by discretizing it to finite elements. To get a correct analysis output, there are several steps to be followed. (i) Elements need to be smooth and continue without sharp edges in the geometry. Otherwise, it may cause discrepancies in the model. (ii) All elements need to be oriented in the same direction. (iii) Size of the element should be a small and more significant number of elements that gives accurate results. (iv) For the symmetrical model, part of the model can be used to analyze the correct constrained application.

2.7.5 Thrust Network Analysis

Thrust Network Analysis (TNA) is a graphic static method for calculating equilibrium solutions for compression-only structures. TNA is also similar to the thrust line analysis. However, thrust line analysis is used for 2-D structures, while TNA can be used for 3-D complex designs to visualize the system's stability and identify possible collapse mechanisms.

This method generates compression-only solutions by assuming that all the loads are applied in the same direction, such as gravitational loads. By manipulating force distribution in the system, it can generate a TNA for the same sets of applied loading. By changing force distribution by using scale factor, can identify the possible thrust network within the shell structure and finalize the optimum height for shell structure. The figure shows the (i) possible collapse due to the tension forces (line of thrust lies outside the section) and (ii) possible safe thrust network analysis (Figure 2-17). Thrust network analysis can be implemented using MATLAB and Rhinoceros 3D (Rippmann and Block, 2012).

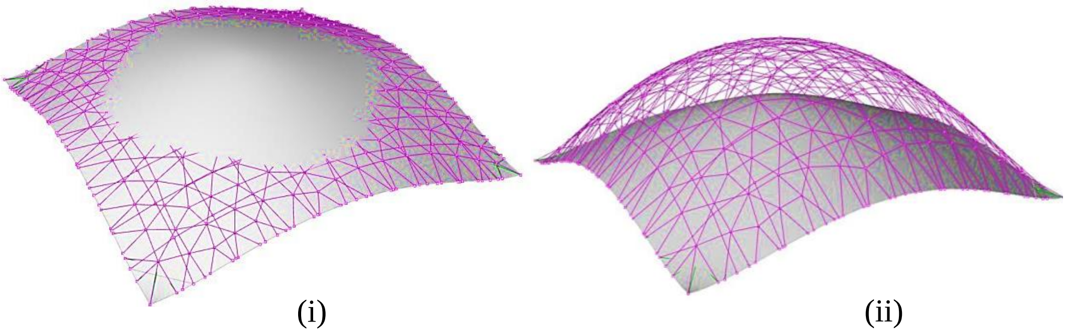

(i) (ii)

Figure 2-17: (i) Possible collapse due to the tension forces and (ii) possible safe thrust network analysis

2.7.6 Grid patterns

Grid patterns are used as a digital discretization of a continuous shell structure. This can be very useful to assemble of shell structures with joints or claddings. These patterns do not represent a force distribution. However, it can be used to construct a surface map, which can be used to control mesh for surfaces and construct a smooth surface. There are two main shapes to be considered when designing patterns, geometrical or topological shapes (Figure 2-18) (Leung, 2018).

Surfaces which modeled with geometrical grid patterns used to achieve feasible structures. However, for optimum and efficient design practices, topographical patterns can be used (Oval et al., 2018).

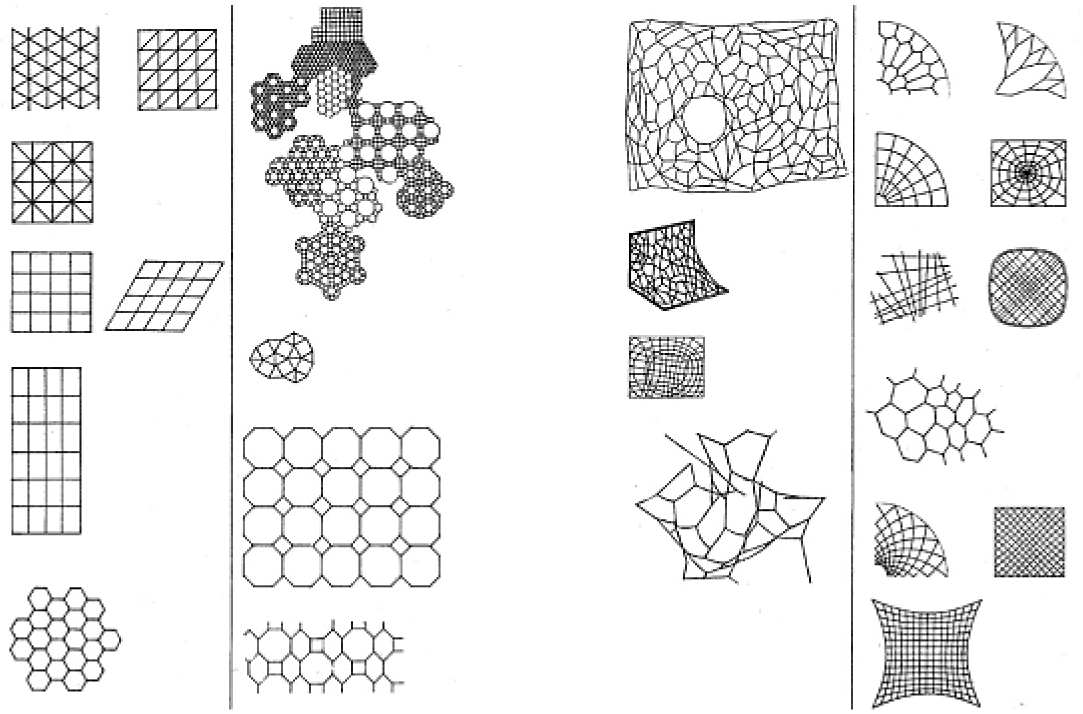

(a) (b)

Figure 2-18: Grid patterns; (a) Geometrical grid patterns and (b) Topology patterns
Source: (Leung, 2018)

2.8 Materials for the construction of shells and vaults

Most common modern shell and vault constructions practice is to use in-situ reinforced concrete due to its high plasticity. However, higher material cost is a main drawback of reinforced concrete. Also, due to the shrinkage and thermal expansions, concrete shells are subjected to form cracks. However, early shell construction practices of thin tile vaulting or even masonry vaulting systems are still use by many other countries.

2.8.1 Reinforced Concrete

Reinforced concrete is the most commonly used material in the construction industry. Félix Candela Outeriño, an Architect (1910-1997) and Heinz Isler, structural engineer (1926-2009), is well known for developing reinforced concrete thin shells using simple forms to complex geometries. E.g. Los Manantiales Restaurant, in Mexico (Figure 2-20), 1958- By Félix Candela, Highway service area Deitingen south, Switzerland, 1968- By Heinz Isler (Figure 2-20) (Chilton and Chuang, 2017).

Although thin shells made from reinforced concrete are strong structural forms, there are few drawbacks in concrete shells. The most common issue is sealing. If not treated correctly, rainwater can seep through the structure since concrete is a porous material.

Figure 2-20: Los Manantiales Restaurant, Xochimilco, Mexico, 1958-Félix Candela
Source: (Chilton and Chuang, 2017)

Figure 2-19: Highway service area Deitingen south, triangle concrete cupola roofs, Switzerland, 1968- Heinz Isler
Source: (Chilton and Chuang, 2017)

Also, when considered the embodied energy, Portland cement is the primary source of embodied energy in concrete (embodied carbon of 0.912 kgCO2e/kg) (Hammond and Jones, 2008). Thus, replacing cement with alternatives will significantly reduce the embodied carbon.

2.8.2 Textile Reinforced Concrete (TRC)

Textile reinforcement is a polymer-impregnated carbon fiber that is knitted into textile meshes to improve the load transfer between fibers and bond characteristics. Also, fiber materials used in TRC are non-corrosive, which gives a massive advantage over typical steel in terms of reduction of self-weight and durability, which will be ideal for shell construction (Figure 2-21). However, the embodied carbon of these fiber materials is much higher than the cement or steel reinforcement (Embodied carbon of Carbon fiber or Aramid fiber is 20.3-17.3 kgCO2e/kg) (Hawkins, 2019).

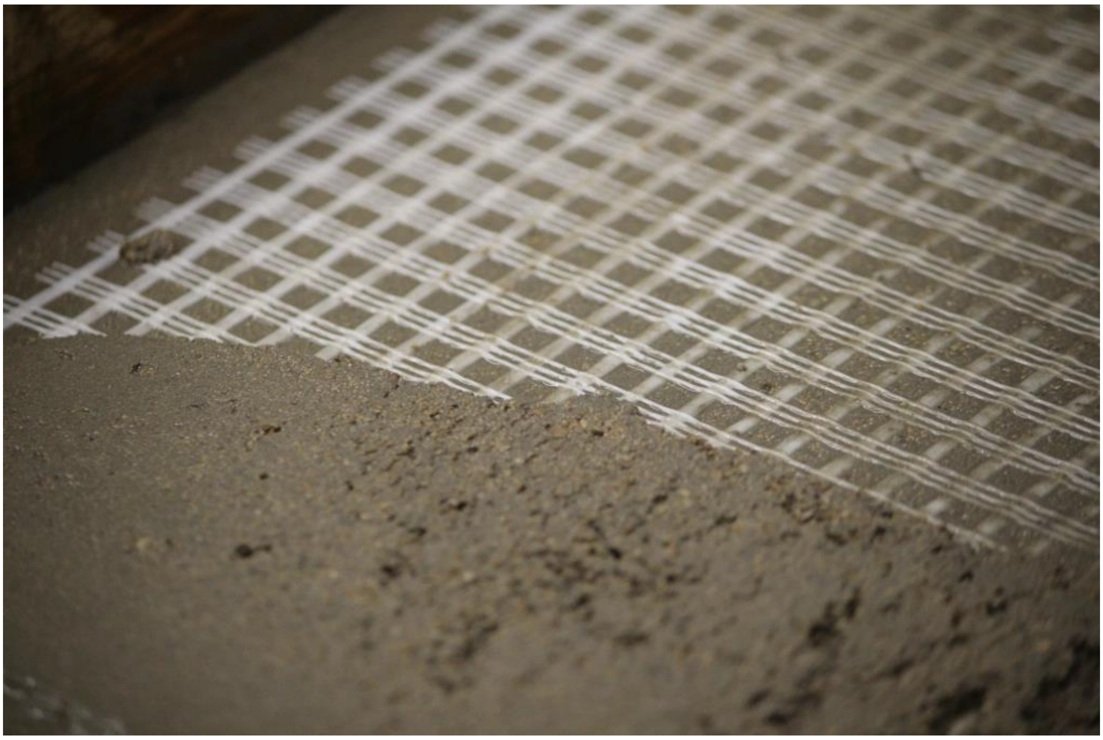

Figure 2-21: Close view of the Textile Reinforced Concrete (TRC)

Source: willhawkinsstructures.wordpress.com

2.8.3 Thin tiles

Thin tiles as a vaulting material are centuries old construction method. Rafael Guastavino Monreo, architect and master builder, implemented the vaulting method to the USA and was particularly active in tile vaulting.

He refines this century-old method as ‘Catalan vaulting’, which involves a technique using thin tiles. This technique is found to be a more effective and sustainable construction technique compared with the traditional construction method. Since this is a lightweight construction, thin tiles create less horizontal thrust than conventional masonry structures. A thin-tile vaulting system requires no formwork (Figure 2-22). To withhold the loading from the form, it requires at least three layers of thin tiles. With a fast-setting binding agent (Normally Plaster of Paris paste can be used) and falsework or guided strings, the first layer of the shell can be constructed. After the first layer, other layers can be applied on top of each succeeding layer using mortar paste and the bottom layer, which will form the top layers. Also, for second and third layers, stronger cementitious mortar can be used (Block et al., 2010).

Figure 2-22: Experimental CSEB Catalan vault with clay mortar
Source: (Smith & Davis, 2016)

Some well-known projects that use vault construction using stabilized earth tiles are Stadium at a cricket stadium in Rwanda, SUDU housing prototype in Ethiopia, and the Mapungubwe national park centre in South Africa (Figure 2-23). These projects were carried out with un-skilled workers and a low level of supervision. These projects are the best indication that vault construction using tiles is a successful method nowadays. The Mapungubwe project and Cricket stadium in Rwanda were highly successful and won various architectural awards due to their aesthetic appearance (Rajabzadeh and Sassone, 2013).

Figure 2-23: Mapungubwe national park centre in South Africa
Source:(Rajabzadeh & Sassone, 2013)

However, there are several drawbacks to this technology. The cost of the construction may comparatively higher specially in developing countries due to its labor-intensive work. Also, significant experiments and testing needed to be carried out to identify suitable soil for the construction. Fast setting mortar required for the construction should also have good binding properties since the quality and purity of these bindings are uncertain, especially in developing countries.

2.8.4 Mud-Concrete (MC)

Mud-concrete is a form of concrete produced using soil, cement and water, an innovative concept developed by Sri Lankan researchers. There are various products that use mud-concrete as the material. E.g. Mud-Concrete Blocks (MCB), Load bearing MC walls (Arooz, 2019), MC Paving blocks (Udawattha et al., 2017), MC Floor finishing (Galabada and Halwatura, 2019).

In Mud-concrete technology, coarse aggregates and fine aggregates in the concrete mix replaced by well-graded soil, which has gravel, sand, and fine particles at required percentages (Figure 2-24) (Arooz and Halwatura, 2018).

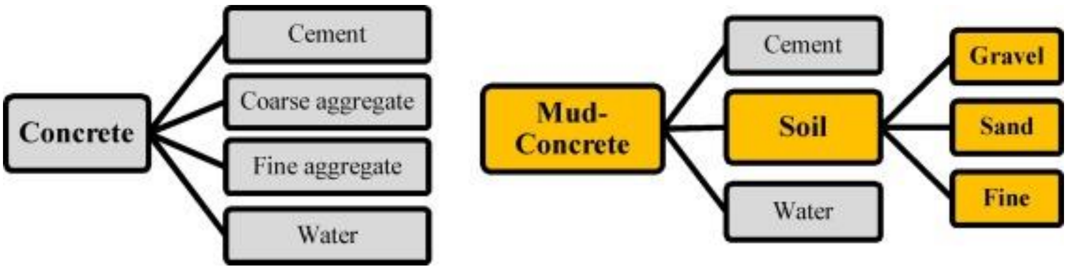

Figure 2-24: Difference between Concrete and Mud-Concrete mixture
Source: (Arooz & Halwatura, 2018)

According to Arooz & Halwatura, 20% of the water from a dry mix of mud -concrete gives a good workable mixture. The mix design for the mud-concrete load-bearing wall was identified as the most suitable mix design rather than the mix design for mud-concrete blocks to achieve good flowability. Therefore, a suitable mud-concrete mix design for the proposed slab system was selected as shown in Table 2-1

Table 2-1: Mud-Concrete mix design for load bearing walls

Soil Proportions	Fine (≤ Sieve size 0.425mm)	5%
	Sand (Sieve size 0.425mm ≤ Sand ≤ 4.75mm)	50%
	Gravel (Sieve size 4.75mm ≤ Gravel ≤ 32mm)	45%
Cement	Minimum cement from total sample weight	4%
Water	Water from dry mix	26-28%

Source: (Arooz & Halwatura, 2018)

2.9 Summary for the literature review

This chapter began by stating the impact of the building construction sector to the climate change and as a solution to the current situation, it proposed sustainable design solution for flooring systems by using earthen materials. Brief discussion on distribution of earthen constructions were discussed then after. Possibility of use of shell structures for sustainable constructions were then discussed with several analysis methods and the suitable materials for the construction were finally discussed.

Key findings from the literature review are given below;

- Earth has been used as the building material in many historical buildings across the world.
- Most of the embodied energy in a typical multi-storey building structure (60% to 70%), exists within the floors. It was identified that; earthen slab system would be huge step towards archiving fully sustainable design.
- Thin-shell structures were identified as potential structural system for slab systems which results reduction in material usage. However, cost of the modern shell constructions is comparatively high. Thus, mud-concrete was found to be a potential material to developed as slab system by incorporating with shells.

3 DEVELOPMENT OF THE THIN SHELL SLAB SYSTEM

3.1 Introduction

This chapter describes the proposed thin shell slab system, including the form finding methods, load analysis and construction process. Analysis was carried out to find the structural behavior of the three different vault structures which has both square and rectangular footprint areas by considering the design floor space. Construction process is explored, while identifying two main formwork systems. The results from the load analysis highlights the key findings to be addressed in discussion.

3.2 Form and form development

Forms can be developed by altering its physical appearance, from flat surfaces to 3-dimentional curved surfaces. These surfaces can be implemented to create lightweight shell structures which achieved its stiffness through its curved surface (e.g. single curvature- Barrel vaults, double curvature- domes and combination of single and double curvatures – freeform structures) (Figure 3-1). (Mansoori et al., 2019)

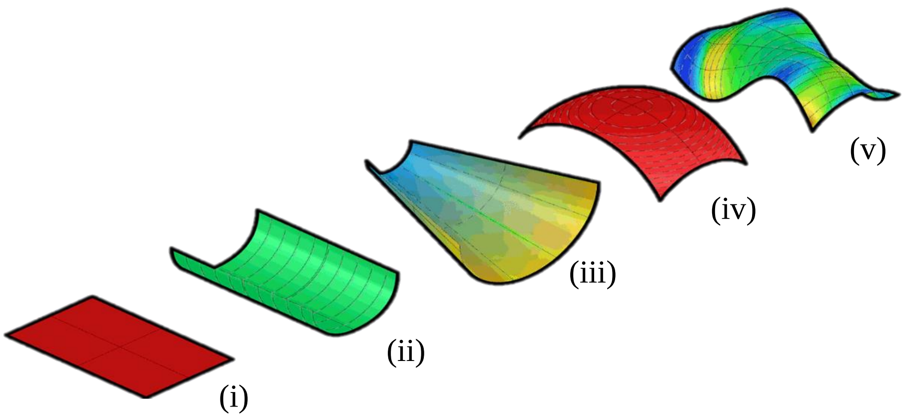

Figure 3-1: Surface typology; (i) flat surface, (ii) singly-curved surface, (iii) conically shaped surface, (iv) doubly-curved surface and (v) freeform surface

Source: (Mansoori et al., 2019)

Thus, by considering the shape and rigidity of the structure, positive doubly curved shell was selected for the proposed design to develop it as a thin-shell slab system. The proposed slab system consists of two main components; shell and ballast loading. Ballast loading, also known as non-structural filling is proposed to improve stability of the structure as well as to see it as a flooring to upper levels (Figure 3-2).

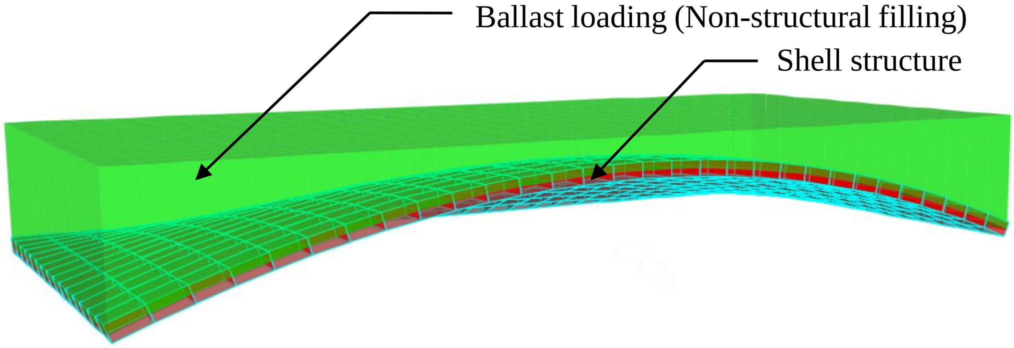

Figure 3-2: Cross section of the proposed slab system illustrating shell and ballast loading

3.2.1 Requirement of reinforcement

The proposed shell should need to be designed as a compression-only structure using positive doubly curved shell. Which means the structure can resist its self-weight and also the external loadings under compression. Thus, the structure will completely depend on this curved shape and the material strength. Normally reinforcements are used to resist the tension developed in a structure made of low tensile strength materials. Since the proposed slab is a compression -only structure, the requirement of reinforcement for the design can be neglected.

3.2.2 Floor leveling

The main structural requirement of the ballast loading is to transfer floor load to the shell structure. For the non-structural filling, any material can be used. However, to further improve the stability and to address the sustainable development, Mud-Concrete mixture is proposed to use in both shell and ballast loading.

3.3 Structural Analysis

The finite element model should be able to properly represent the physical properties as well as the linear-elastic behavior of masonry structure. Thus, by considering the elastic material behavior, linear analyzing method was conducted using Finite Element Software "SAP2000" to analysis of the proposed masonry structure.

3.3.1 Structural Requirement

Column to column distance (clear span) of 3m is typical for Sri Lankan housing unit. Therefore, for the doubly curved shell structure, 3m x 3m square footprint area and 6m x 3m rectangular footprint area were selected as initial geometries. However, for the initial design purposes and ease of construction purposes 1m x 1m footprint area was also selected.

3.3.2 Form finding- Generating coordinate system for funicular shell

The coordinates for the funicular shells were determined by using the given formula extracted by the (*IS 6332 (1984): Code of practice for construction of floor and roofs using precast doubly-curved shell units*, 2000)(Figure 3-3). For all geometries, the size of the grid was selected as 100mm.

$$Z = \frac{Z_{max}}{a^2 b^2}(a^2 - x^2)(b^2 - y^2) \tag{2}$$

Where;

- Z = Vertical ordinate at point x, y;
- Z_{max} = Maximum central rise;
- a = Half length of the shell;
- b = Half width of the shell;
- x, y = The coordinates of the grid point from the origin, which is taken as the center of the shell unit

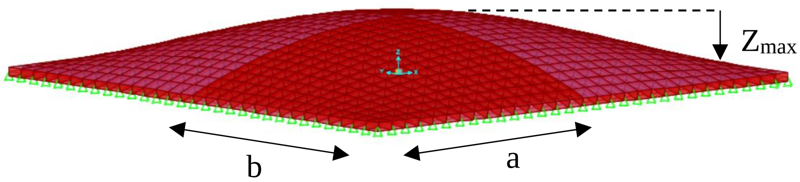

Figure 3-3: Parametric definition for the shell structure

3.3.3 Materials Characterization

Shell structure is a thin curved compression-only structure which perform well under external loading without deforming its shape. For the design, shell was defined as thin shell structure and end restraints were fixed as pinned supports using structural analysis and design software -SAP2000.

Ballast loading is a non-structural filling, which used for stabilization of the structure and to see it as a floor. For analyzing, ballast loading was model in SAP2000 as solid elements. Material for the design was considered as Mud-Concrete. Thus, Mud-Concrete properties were defined for both shell and ballast loading. Soil characterization data was taken from the paper “Structural Analysis of Tile Vaulting: Method and Variables” by David López López which is turn borrowed from Atamturktur and Guastavino (López et al., 2014). The density of the Mud-Concrete was extracted from the paper “Mud-concrete block (MCB): mix design & durability characteristics” by Arooz and Halwatura (Arooz and Halwatura, 2018).

Table 3-1: Material input data for the SAP2000

Young’s Modulus (E)	7400	MPa	(López et al., 2014)
Poisson’s Ratio (ν)	0.26		(López et al., 2014)
Density (ρ)	3.3	kN/m^3	(Arooz, 2019)

The combination of both shell and ballast loading is defined as ‘the slab’. For analyzing purposes, loads are applied on directly on top of the ballast loading or in other words, directly on top of the vault section (Figure 3-4).

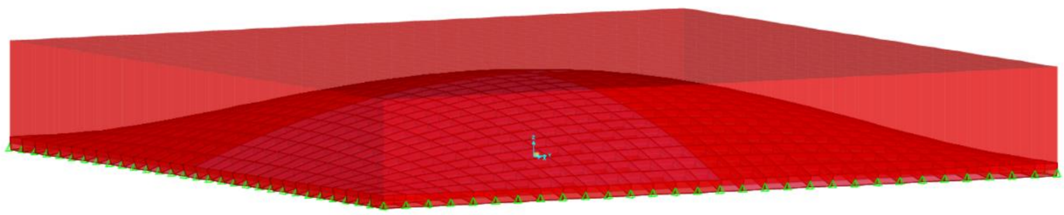

Figure 3-4: Funicular shell with ballast loading

3.3.4 Parameter 1- Define grid pattern and grid spacing

In this study grid configuration was designed as square grid pattern. Since the boundary condition is square or rectangular shape, to fill the boundary without introducing asymmetries to the design square grid pattern was selected (Figure 3-5).

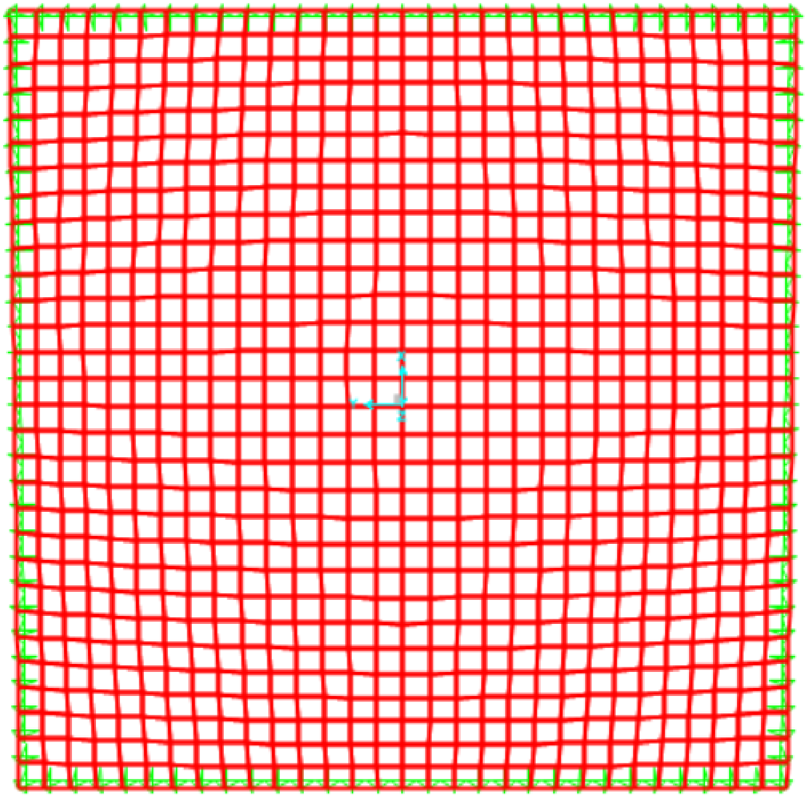

Figure 3-5: Rectangular shape grid of the shell

To find the most suitable grid spacing for the design, 3m x3m shell was analysis by manipulating various grid spaces to identify the stress developed in the bottom face of the shell using SAP2000 (Table 3-2).

Table 3-2: Suitable grid spacing for 3m x 3m shell structure

Grid Size	**S_{Max} Bot in N/mm^2**	
mm	**Compression**	**Tension**
375	0.093	-0.03000
187.5	0.032	-0.00600
100	0.021	-0.00460
75	0.017	-0.00370
50	0.012	-0.00260
25	0.006	-0.00140
10	0.0023	-0.00067

According to the grid analysis data, finer grid patterns give much better results. However, due to the complexity of the analysis for finer grid patterns, a medium grid size of 100mm x 100mm grid was selected for the design.

3.3.5 Parameter 2- Selecting shell thickness

The shells were modeled with dimensions mentioned in Table 3-3 to identify the optimum shell thickness for the design. The initial rise of the shells was taken as L/10, where L is the span of the shell while the end support restrained was fixed as pinned joints (Figure 3-6).

Table 3-3: Identifying suitable shell thicknesses for shell structures

Geometry of the Shell	Vault plan dimensions in mm	Shell thickness in mm	Rise in mm	S_{Max} Bot in N/mm^2
Square	1000 x 1000	25	100	-0.121
	1000 x 1000	50	100	-0.057
	1000 x 1000	75	100	-0.034
	1000 x 1000	100	100	-0.023
Square	3000 x 3000	25	300	-0.192
	3000 x 3000	50	300	-0.057
	3000 x 3000	75	300	-0.019
	3000 x 3000	100	300	-0.005
Rectangle	6000 x 3000	25	600	-0.166
	6000 x 3000	50	600	-0.051
	6000 x 3000	75	600	-0.017
	6000 x 3000	100	600	-0.004

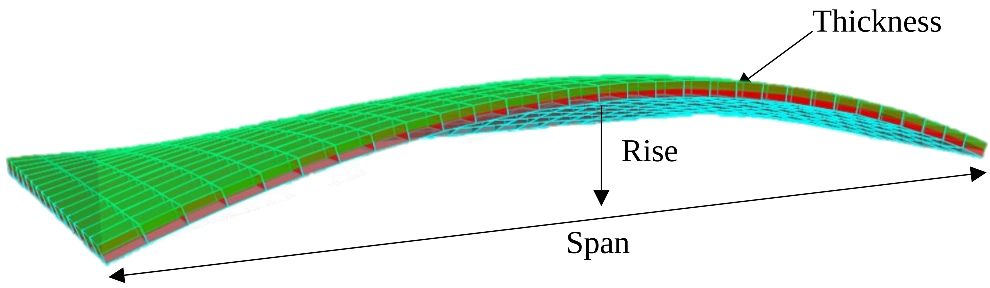

Figure 3-6: Shell terminology

From observation from previous research, it appears that different failure modes exist or even co-exists (mainly buckling failures and shear failures). Since the analyzing model is compression only doubly curved shell structure with a ballast loading, shear failure is the most prominent failure mode. Thus, analysis is carried out to find the tensile stresses developed at the bottom face of the shell structures due to various loading conditions acting on the shell and the ballast loading.

Ballast loading thickness of 50mm from the apex was selected as nominal thickness for all the types by considering the maximum aggregate size of the mud-concrete mixture.

3.3.6 Analysis for Load cases

For two different slab sections (square and rectangular) , possible live loading patterns were analysed individually to determine the critical loading scenario. Impose load was taken as 2.0kN/m^2 according to BS-EN-1991-1. All the loads were applied on the ballast loading on each load cases, and live load area were outlined in bold as shown in Figure 3-7 and Figure 3-8. Maximum compressive stress and tensile stresses at the bottom face of the vault for different load cases are shown in Table 3-4 and Table 3-5.

The stress distribution of the bottom part of the shell shows that live loading applied over one half of the vault (LC-03) gives the maximum stress distribution for the 3m x 3m vault section, while for the 6m x 3m, live loading applied (i) over entire section (LC-01), (ii) over one half of the vault (LC-03), (iii) over three-quarters of the vault (LC-04) gives the maximum stress distribution. However, for the 1m x 1m vault section, maximum stress distribution gives when live loading is applied (i) over the entire section (LC-01) and (ii) over three-quarters of the vault (LC-04).

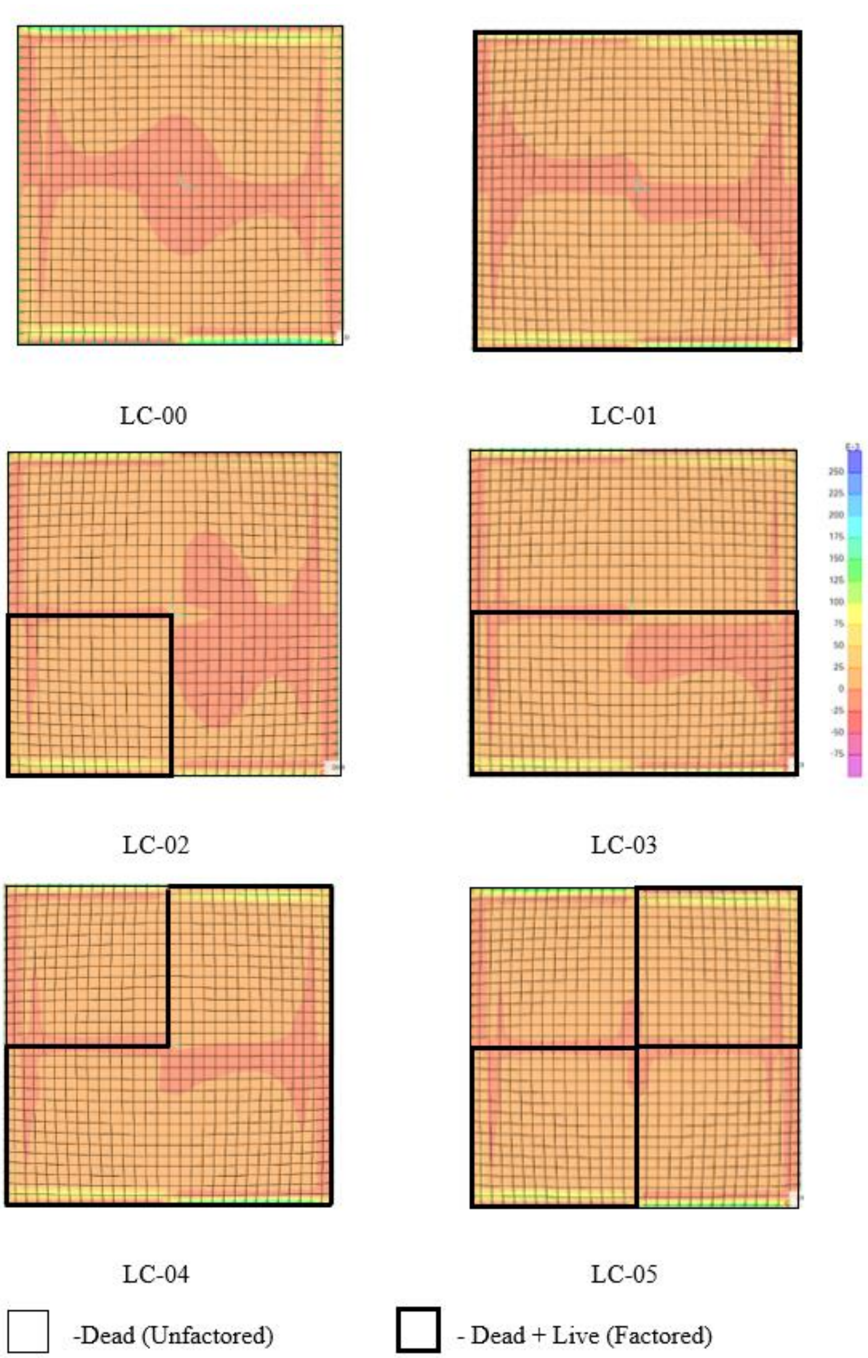

Figure 3-7: Stress distribution across the 3m x 3m shell at the design loading for each live loading patterns while live load of $2kN/m^2$ outlined in bold

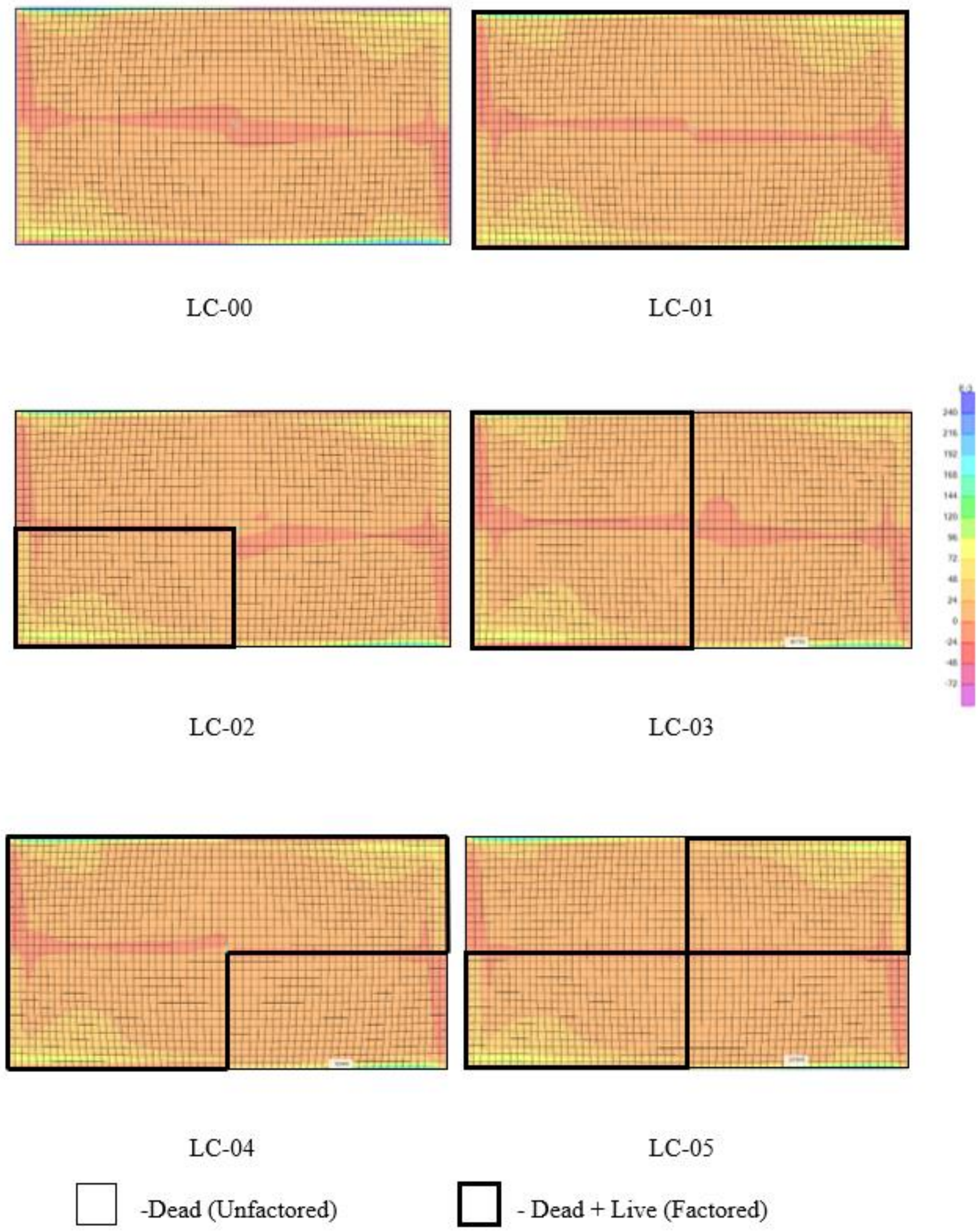

Figure 3-8: Stress distribution across the 6m x 3m shell at the design loading for each live loading patterns while live load of $2kN/m^2$ outlined in bold

Table 3-4: Load case analysis for 3m x 3m shell with ballast loading

Load Case	Maximum tensile stress	Maximum Compressive stress
	N/mm^2	N/mm^2
LC-00	0.059	0.153
LC-01	0.072	0.179
LC-02	0.091	0.232
LC-03	0.094	0.231
LC-04	0.093	0.231
LC-05	0.062	0.16

Table 3-5: Load case analysis for 6m x 3m shell with ballast loading

Load Case	Maximum tensile stress	Maximum Compressive stress
	N/mm^2	N/mm^2
LC-00	0.063	0.192
LC-01	0.087	0.256
LC-02	0.081	0.239
LC-03	0.087	0.256
LC-04	0.087	0.256
LC-05	0.081	0.239

3.3.7 Analysis for concentrated live loading

For critical live loading, 2kN loading was selected as concentrated live loading according to (*EN 1991-1-1: Eurocode 1: Actions on structures - Part 1-1: General actions - Densities, self-weight, imposed loads for buildings*, 1991). The analysis is conducted based on considering the collapse mechanism of the vault section. Thus, concentrated point load was applied along each grid point to analysis the maximum tensile stresses and compressive stresses (Figure 3-9 to Figure 3-12).

Concentrated loading should need to be applied over a square with a width of 50mm. However, for the analyzing purpose, concentrated point load was directly applied over the grid point on the ballast loading. Since loading was applied on the ballast rather than the shell structure, the effect was assumed to be negligible.

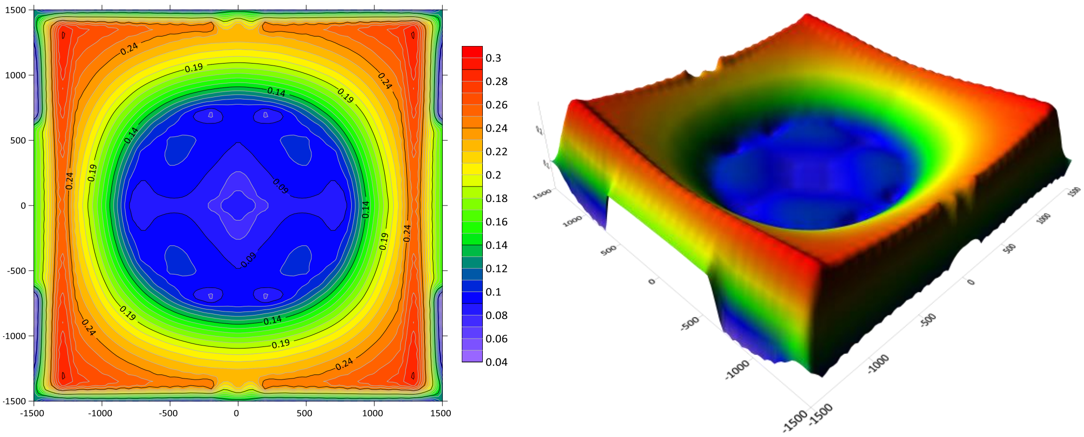

Figure 3-9: Tensile stress distribution of 3m x 3m vault, when the concentrated point load of 2kN acting on each grid point
(Illustrated with Surfer16)

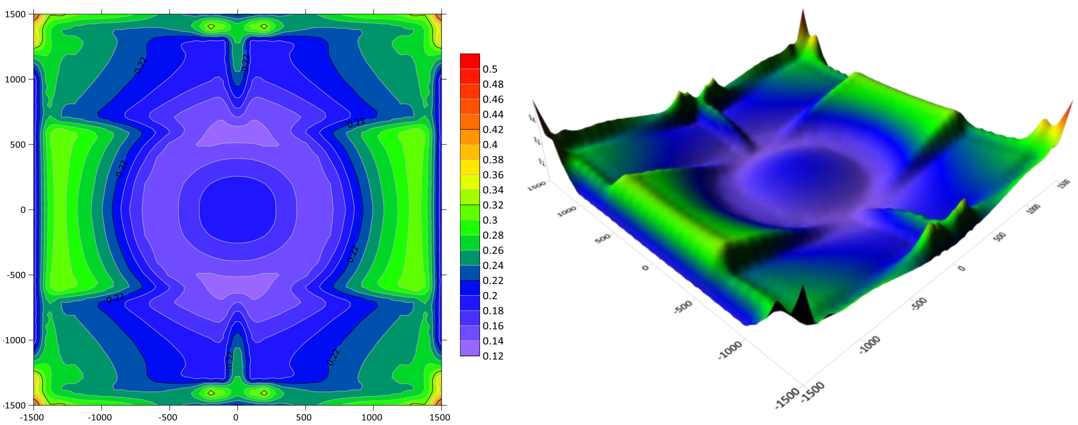

Figure 3-10: Compressive stress distribution of 3m x 3m vault, when the concentrated point load of 2kN acting on each grid point
(Illustrated with Surfer16)

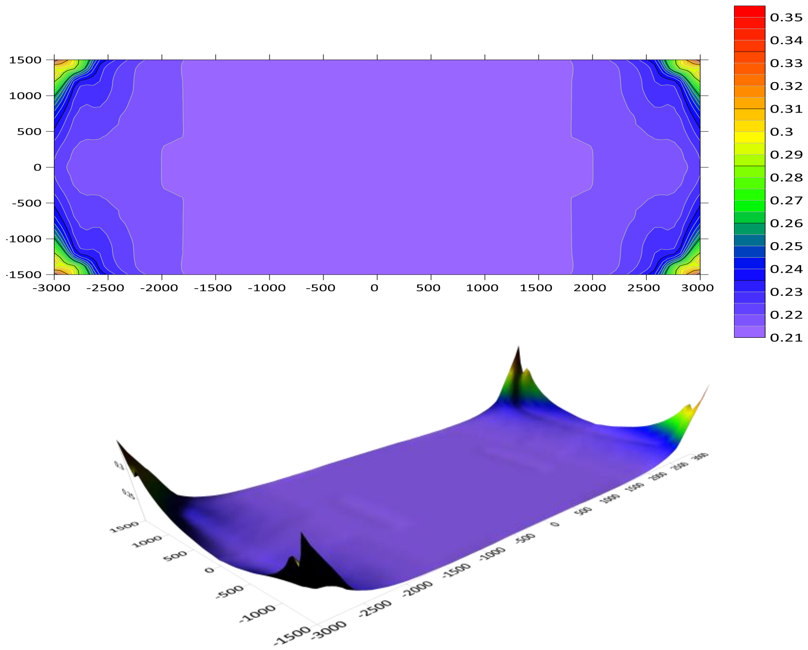

Figure 3-11: Tensile stress distribution of 6m x 3m vault, when the concentrated point load of 2kN acting on each grid point
(Illustrated with Surfer16)

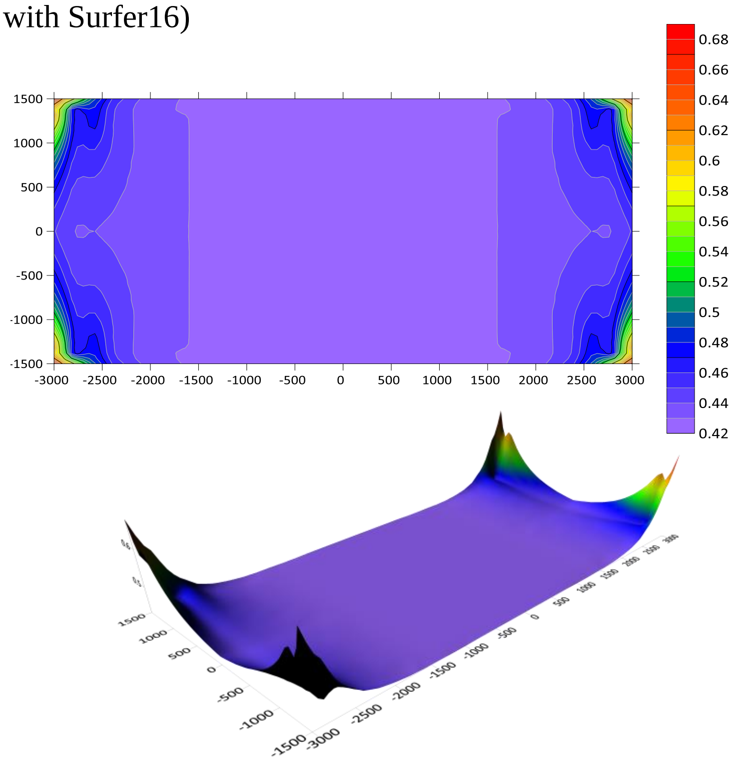

Figure 3-12: Compressive stress distribution of 6m x 3m vault, when the concentrated point load of 2kN acting on each grid point
(Illustrated with Surfer16)

3.3.8 Lateral thrust distribution at the supports

It is essential to identify the other failure mode due to the movement of the supports. It could be a result due to the horizontal load as a support reaction force. Thus, this is a critical factor to be considered.

For the fully loaded vault sections (LC-01), horizontal and vertical stress distribution of each side were plotted accordingly (Figure 3-13 to Figure 3-18).

For the 3m x 3m and 6m x 3m vault sections, maximum horizontal and vertical stresses occur at the mid span of the supports. Therefore, if the supports were inadequate to withstand the loading or to prevent failure due to the movement of the supports, increasing the thickness of the wall would be ideal solution.

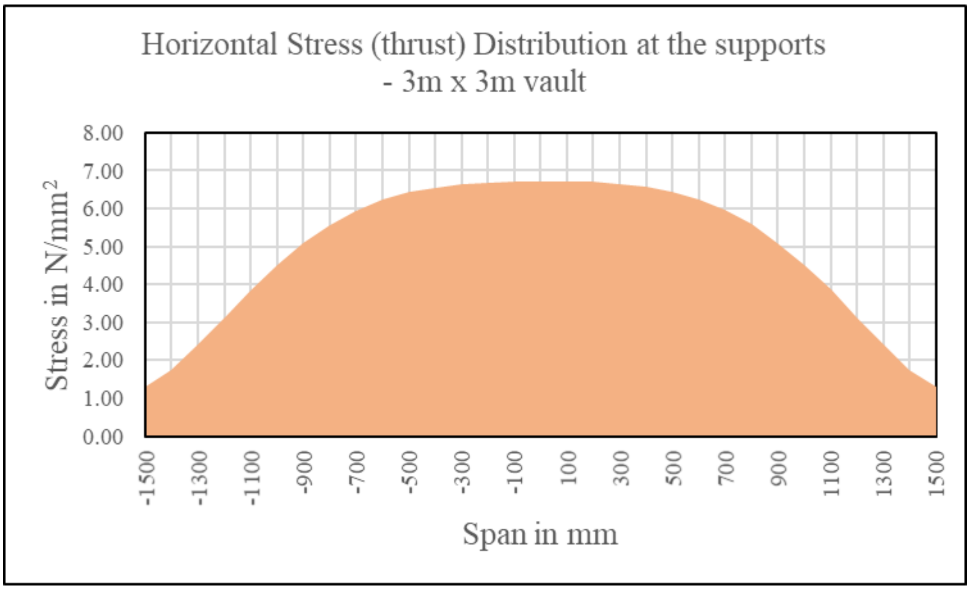

Figure 3-13: Horizontal stress (thrust) distribution of 3m x 3m vault at the supports

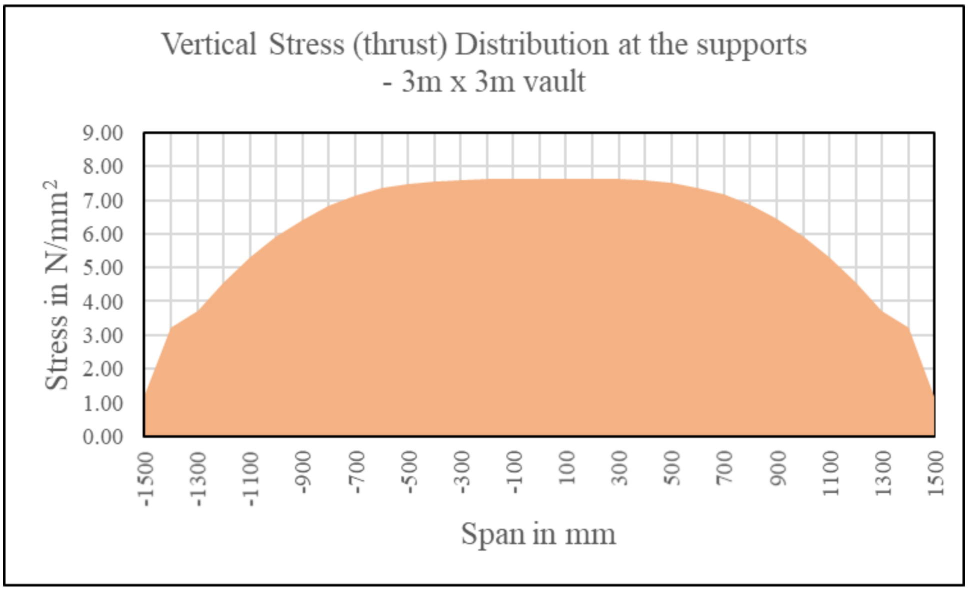

Figure 3-14: Vertical stress (thrust) distribution of 3m x 3m vault at the supports

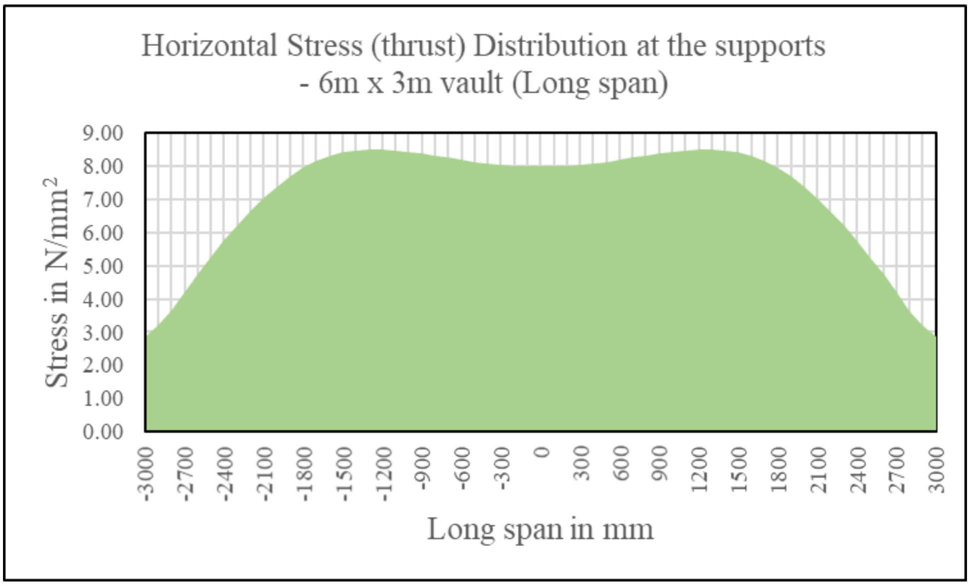

Figure 3-15: Horizontal stress (thrust) distribution of 6m x 3m vault at the supports (Long span)

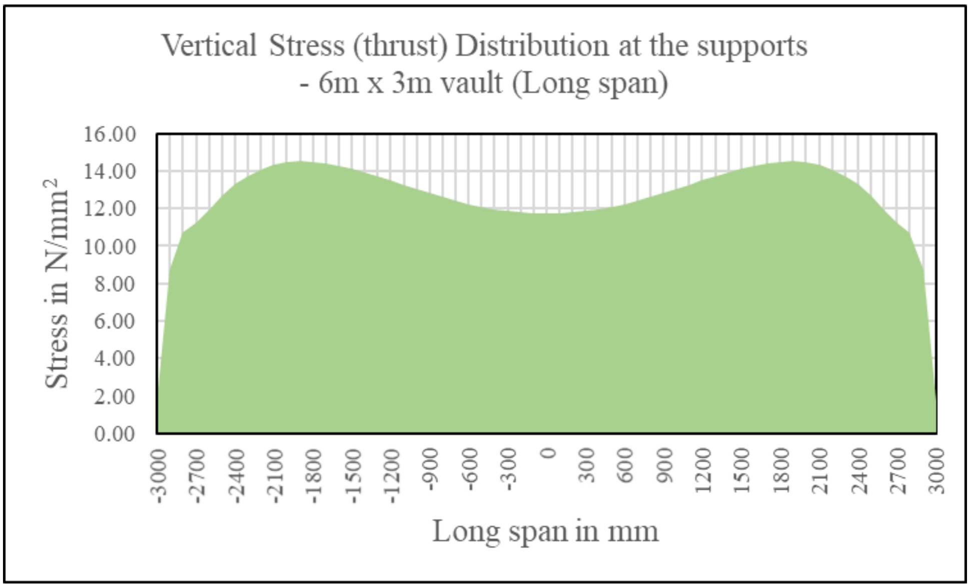

Figure 3-16: Vertical stress (thrust) distribution of 6m x 3m vault at the supports (Long span)

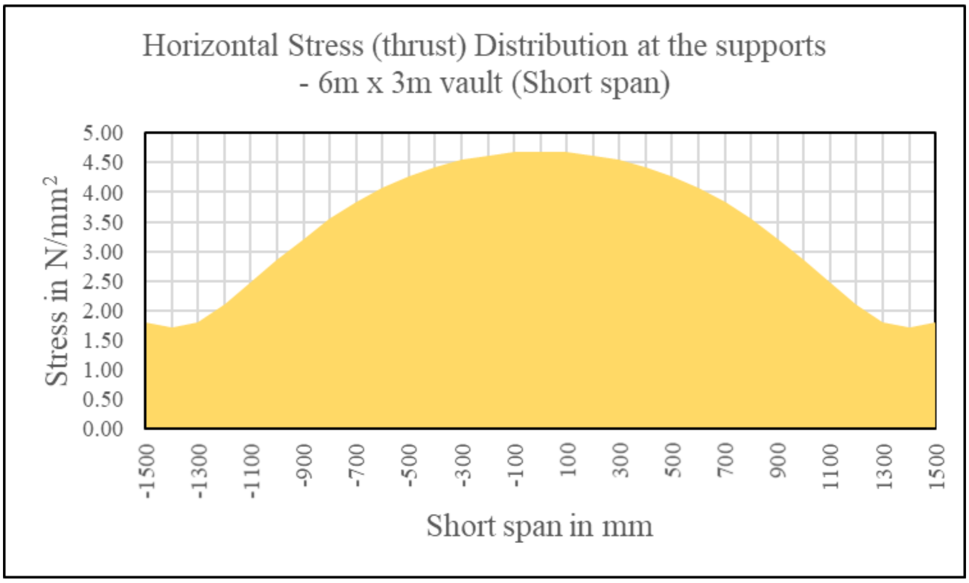

Figure 3-17: Horizontal stress (thrust) distribution of 6m x 3m vault at the supports (Short span)

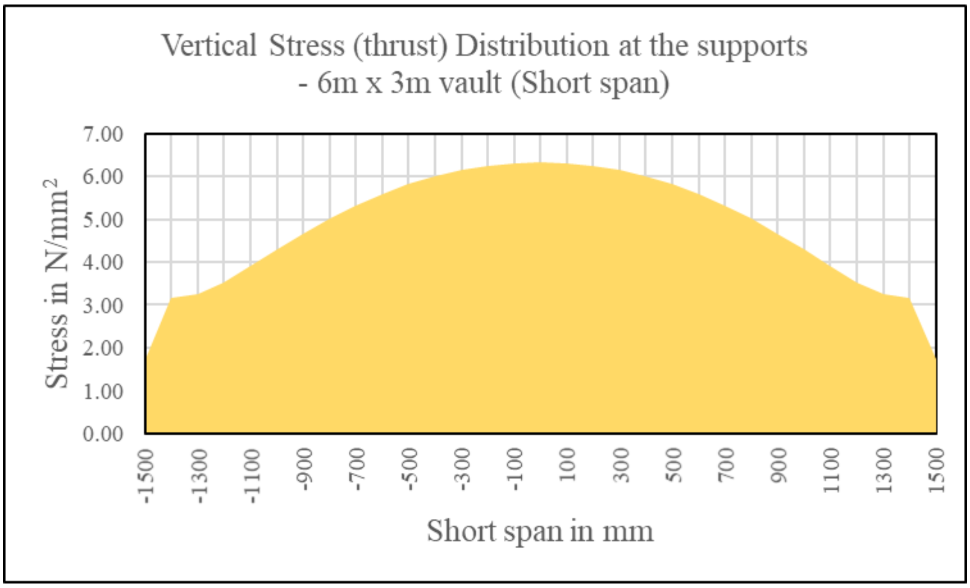

Figure 3-18: Vertical stress (thrust) distribution of 6m x 3m vault at the supports (Short span)

3.4 Construction of the doubly curved shell structure

To validate the structural analysis, experimental test should need to conduct for full-scale structure. However, due to relatively high cost and resources, a 1m x 1m -scaled structure was proposed to construct.

3.4.1 Preliminaries (wall/beam setup)

As the initial step, setting out work conducted. Then after, 1m hight wall section was constructed with 0.5m opening at both ends. The wall segments were designed to have openings at both ends to mimic the actual room (Figure 3-19) (Also, these opening are

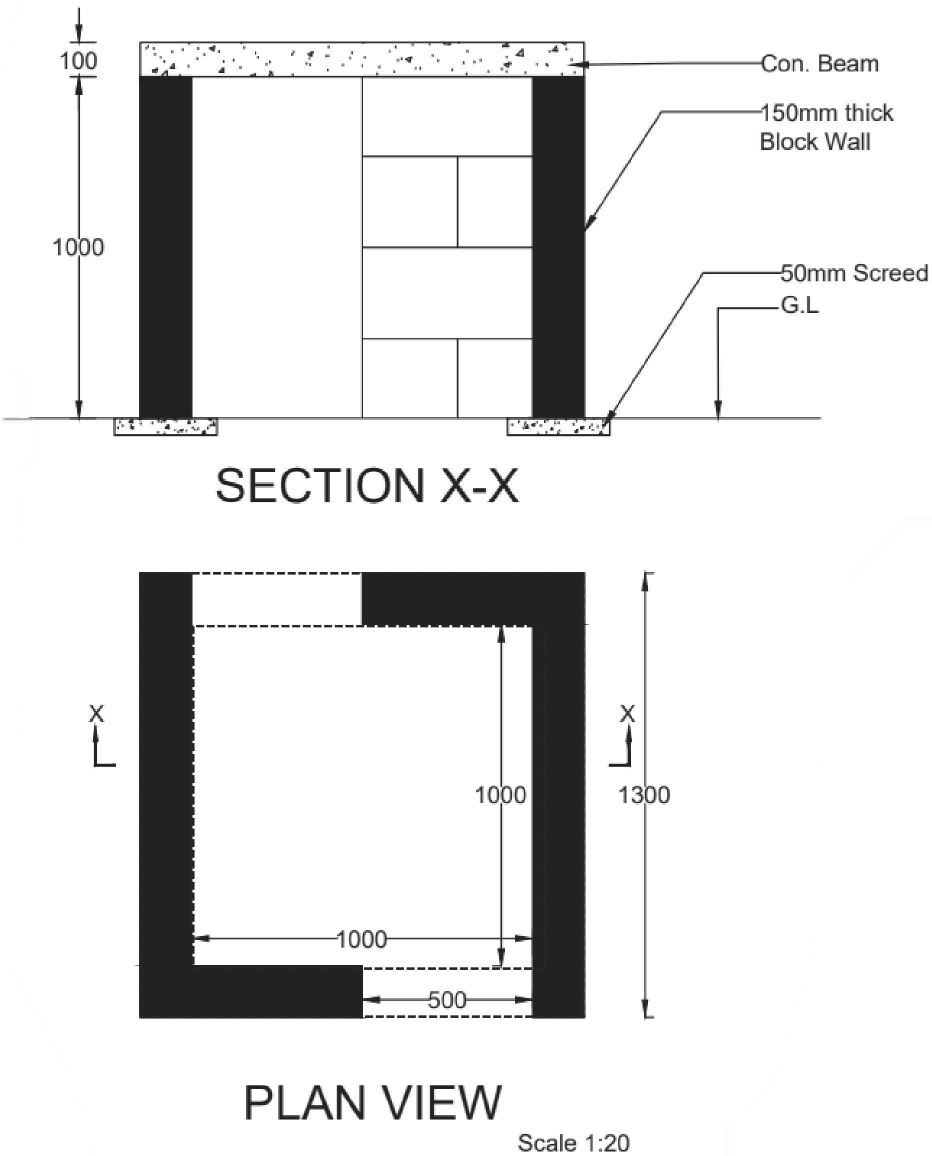

Figure 3-19: Detailed drawing for the wall and beam setup

required to construct the formwork and to provide supports). Thus, concrete beam is required to withstand the upper loading. Figure 3-20 shows the constructed wall segments setup.

Figure 3-20: Setting out & construction of wall segments

3.4.2 Formwork design and construction

To design the formwork, Rhinoceroses 3D software was used with Grasshopper Add-on. Initially, two possible formwork system were proposed for the design. (i) waffle type formwork which can be construct with steel plates and (ii) plywood formwork system, cut into desired shapes to cast masonry cement mould on it (Figure 3-21).

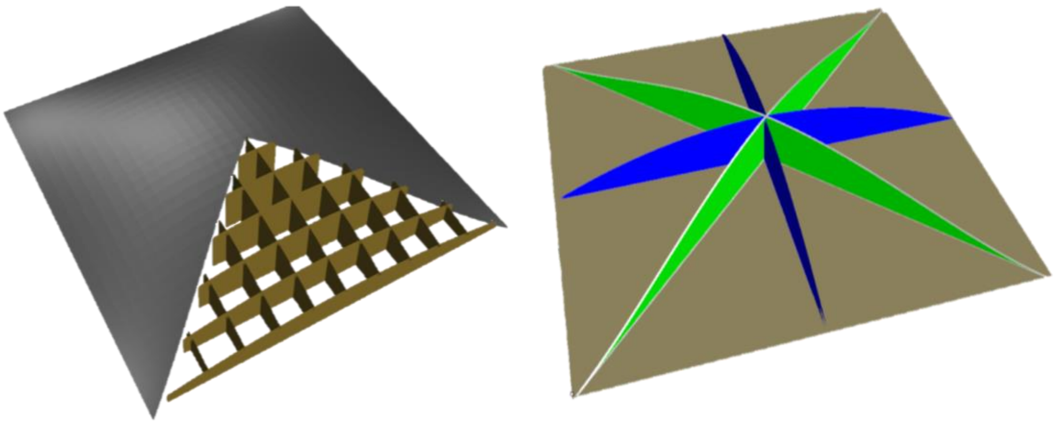

(i) (ii)

Figure 3-21: (i) Waffle type steel formwork & (ii) Plywood formwork (Software: Rhinoceros 3D)

The masonry mold method was used to get the funicular shell shape by considering the ease of construction. For the construction, 12mm thick plywood boards were used to get the desired shapes for the skeleton of the formwork. Generated funicular shell model (SAP2000) was used as guidance to create the arch-shaped segments and placed them accordingly to get the 100mm rise for the shell structure, as shown in Figure 3-22.

Figure 3-22: Arch shaped segments fixed to the formwork to get the desired shape

After fixing the formwork in place using props, cement mortar (1:8) was used to finish the surface, as shown in Figure 3-23.

Figure 3-23: Finished surface with cement mortar

3.4.3 Material preparation

Three different soil samples were collected from different locations, and sieve tests were carried out to find the most suitable soil for the construction. Collected soil samples are showing in Figure 3-24.

Soil sample I Soil sample II Soil sample III

Figure 3-24: Collected soil samples

By considering the sieve analysis, "Soil sample I" was selected for the construction. Since the selected soil sample has 44% gravel and 46% of sand particles (see Appendix B). Thus, it was identified as the most suitable soil sample for the design. Collected soil was then air-dried and sieved through 32mm, 4.75mm, and 0.425mm sieves to obtain the required soil proportions for the Mud-concrete mixture. The quantity of required soil was calculated in the weight. Figure 3-25 shows the soil proportions during the mixing stage.

Figure 3-25: Soil proportions for the mixture

3.4.4 Required soil proportions for the construction

- Compacted volume of soil (Approx.) = $0.15\ m^3$
- Required loose soil volume = $0.15m^3$ x 150% = $0.225m^3$
- Wastage (+25%) = $0.225m^3$ x 125% = $0.282m^3$
- Required total volume = $0.30m^3$

Take the density of soil as $1900kg/m^3$ and density of cement as $1440kg/m^3$ (Jayasinghe, 2011)

Therefore;

- Required fine particles (5%) = $0.015m^3$ = 28.5kg
- Required sand particles (45%) = $0.135m^3$ = 256.5kg
- Required gravel particles (50%) = $0.150m^3$ = 285.0kg
- Required water (20%) = $0.060m^3$ = 60l
- Required cement (4%) = $0.012m^3$ = 17.28kg

- Admixtures = Water reducer (0.6%-1.5% from cementitious materials)

An admixture (water reducer) can be used to improve the workability of the design mix without using an excessive amount of water. Apart from improving the workability, this will reduce the segregation as well as bleeding of the concrete. The admixture should be added to the damp concrete after the 60%-80% mixing water is added to achieve an excellent plasticizing effect.

3.4.5 Summary of the construction process

Construction sequence for the construction of doubly curved shell structure as follows.

(i) Setting out and construction of wall segments and beam

(ii) Placing the shuttering

(iii) Fixing the shuttering with props/struts and folded wedges – Timber props/struts and folding wedges were used for the construction (Figure 3-26)

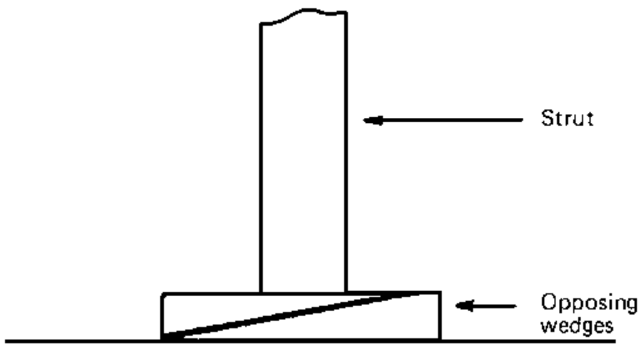

Figure 3-26: Use of opposing wedges to tension the strut in position
Source: Natural Disaster Organization, 183 p.)

(iv) Construction of cement mould shell

(v) Fixing sideboards and supports

(vi) Preparation of the finished mould- Oil and grease mix coating applied over the cement mould as a releasing agent.

(vii) Pour wet mud-concrete mixture over the cement mould- Pour wet mud-concrete mixture over the cement mould- In this stage, pour the concrete mixture to the four edges equally and gradually fill over the cement mould. The main reason for this step was to reduce the effect of variable loading conditions, resulting in deformed cement mould.

Vault construction is a two-step method. (i) Construction of shell with the thickness of 50mm and (ii) Construction of ballast filling (thickness is 50mm from the apex). During the shell construction step, the gauge should be used to measure the shell thickness of 50 mm, and after pouring the ballast, the top surface should need to be leveled accordingly (Figure 3-27).

Figure 3-27: Construction sequence for the doubly curved shell structure

3.4.6 Curing & decentring of formwork

Sideboards were removed after 24 hours, and curing was carried out for 21 consecutive days to achieve full strength. As a curing method, the ponding method was used. Small shallow two ponds were prepared on the top of the surface using sand and clayed soil. After that, water was filled up to depth of 50mm. The sides were also covered in canvases and both are kept continuously wet for 21 days.

After the curing is completed (Figure 3-28), the structure was left to dry for another seven days. The lever and wedge methods were used to decentring the formwork. Gradually and without causing sudden shocks to the structure, props were decentred with the cement moulding.


(i) (ii)

Figure 3-28: (i) Completed earthen thin shell slab system & (ii) underside of the slab after erecting the formwork

3.5 Material testing - tensile strength of Mud-Concrete

In a practical scenario, soil-based materials or products have low tensile strength compared to concrete. Since the slab construct without any reinforcement, tensile stresses may develop due to the various loading and leads to tensile cracks. Also, soil-based materials may experience dry shrinkage and cracks due to the presence of finer partials. For Mud-Concrete, mix design was formulate to minimize the shrinkage and to achieve adequate strength. However, it was not tested for tensile strength. Although, the material itself should have the tensile strength to some extent.

Thus, an indirect split tensile test was proposed to determine the tensile strength of the mud-concrete mix. The direct split tensile test has few problems, such as applying axial loads and stresses induced to grips (specimen may break at its ends).

3.5.1 Sample preparation

Total number of six cylindric test specimens were cast for testing (three samples from each batch). For the testing, the length of the specimens should not be less than the diameter and not more than twice the diameter. For the testing, 60mm in diameter and 120mm long test specimens were prepared accordingly.

3.5.2 Sample testing

The tensile splitting test was conducted in accordance with BS-EN-12390-6 after 30 days of curing. The load was applied continuously at a steady rate of $0.05 N/mm^2$ until the sample fails. The tensile splitting strength was recorded at the failure and tensile strength was calculated as shown in the Table 3-6.

Equation 3 was employed to calculate the splitting tensile strength.

$$T = \frac{2\,F}{\pi\,L\,d} \tag{3}$$

Where;

T = The tensile splitting strength (MPa);

F = Maximum applied load (N);

L = The length of the line of contact of the specimen (mm);

d = The designated cross-sectional dimension (mm).

Figure 3-29 shows the split tensile test procedure before and after the load has applied to the specimen and initial crack formation along the axis.

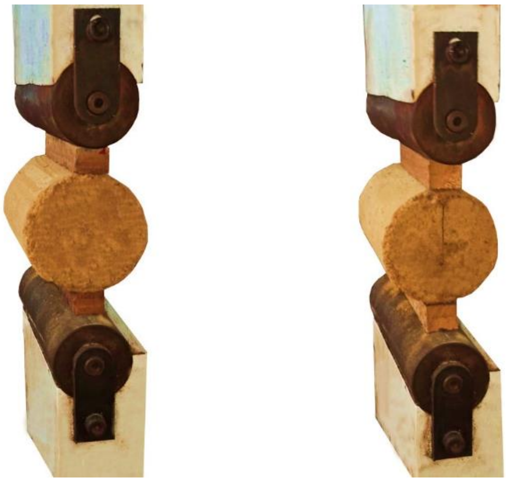

(i) (ii)

Figure 3-29: Split tensile test shows (i) before the load applied to the specimen and (ii) initial crack formation along the axis

Table 3-6: Observation and test results of the tensile splitting test

Sample No.	Applied Load (N)	Length (mm)	Cross-sectional diameter (mm)	Tensile splitting strength (N/mm^2)
S1	1100	120	60	0.09731
S2	950	120	60	0.08404
S3	1050	120	60	0.09289
B1	1100	120	60	0.09731
B2	950	120	60	0.08404
B3	1100	120	60	0.09731

The mean tensile strength was calculated as $0.0951N/mm^2$. According to the structural analysis, the maximum tensile stress which the structure could withstand was identified as $0.093N/mm^2$ during the load case analysis. However, development of tensile stresses will not cause total collapse of the slab system. That would require a crack across full thickness of the slab system to form an admissible collapsing. This will only showcase the lower bound of the collapse loading. Thus, this slab system would be safe for the analysed load cases.

3.6 Strength evaluation of the slab system with physical load test

A load testing on the proposed structure is essential to determine the serviceability of the slab system to verify the structural analysis. Physical load test was conducted after 90 days of the completion of the slab system. Thus, the slab system considered as functionally stable.

Before conducting the load test, underside of the vault section was painted in white to observe the possible crack patterns formed under the vault section.

3.6.1 Load arrangement for physical load test

With structural analysis, initial crack patterns may form at the mid-underside of the structure. Therefore, load need to be applied at the location where the assumed maximum defects occur. Uniformly distributed load was considered to evaluate the performance of the slab system. A set of cement blocks, each weighted approximately 12.5kg were considered to use for the load testing to achieve consistent loading.

3.6.2 Load intensity for the physical load testing

According to the BS-EN-1991-1, for a domestic and residential building floor system, impose load of 2.0 kN/m^2 is typical. Thus, the total test load should need to be larger than that value by considering the serviceability limit state.

3.6.3 Loading procedure

Initially, total number of 22.5 cement blocks were carefully placed on the top surface of the slab system, without loading to the edge beams. During the loading stage, cement blocks were placed near corner edges and then the mid-section to avoid unnecessary loading conditions. After the first layer completed, second layer of cement blocks were stacked on top of the first layer and observed for any crack formation underside of the slab system. Similarly, total number of 7 layers of cement blocks were stacked on top of the slab system without showing any crack formation or any visible deformation. Figure 3-30 shows the loading procedure for the slab system.

Figure 3-30: Loading procedure for the prototype

3.6.4 Results

Nearly, total number of 157.5 cement blocks were stacked on the top of the slab system. This corresponding to a stress of 20.69kN/m^2 without showing visible crack patterns or visible deformation. Therefore, 20kN/m^2 was considered as the safest lower bound limit for the slab system.

3.6.5 Discussion of results

The thickness of the constructed prototype was selected as 100mm from apex. However, nominal thicknesses at the apex point for other vault types such as 3m x 3m and 6m x 3m were also selected as 100mm. The main criteria for selecting nominal thicknesses were identified as size of the aggregates in mix design and the construction sequence. For the vault construction, shell and ballast loading was constructed separately. Thus, for each component constructed with 50mm thickness at the apex.

It was identified that the constructed prototype could withstand more than 10 times of design loading condition. In an actual design, this would be an over design. Since the thickness is not proportionally enlarged with the structural size, overall strength of the actual scale model could be brought down to an optimal value.

3.7 Summary, findings and conclusions

This chapter has introduced the thin shell slab system proposed in the dissertation. The basic shape and behaviour of the structure were identified, allowing to select an ideal size and thicknesses for a typical slab system. More thorough investigation was then carried out using linear FEA. Three different shell sizes were modelled and compared with various thicknesses and heights to identify the structural behaviour of each model. This chapter is also discussed the design, construction and testing of prototype slab system. Challenges concerning practical construction and testing have been addressed and detailed.

The key findings are summarized below:

- Preliminary results indicate that the most suitable thickness for each shell and ballast loading as 50mm thickness from the apex.

- Asymmetric live loading is critical for these types of shells. Most prominent asymmetric loading for larger sections were identified when the load is applied over half of the span.
- A masonry cement mould with framework would be ideal small constructions, to get the correct doubly curved shell shape of the underside of the structure, while for modular constructions a steel formwork would be more suitable.
- For the construction process, it is ideal to fill the shell component first and then filling the ballast loading to an indicated level. Since the total load of the filling will act as evenly across the formwork.

Peak stresses are concentrated at the mid-span of the slab system for smaller size vaults, since the edge beams and walls act more rigidly for the slab system. However, for larger rectangular or square sections, peak stresses are concentrated at the four edges.

4 ENVIRONMENTAL AND ECONOMIC PERFORMANCE

Various aspects need to be considered when comparing the cost, such as floor size, ease of construction, material availability, availability of workforce, transportation.

In this chapter, the comparative cost for (i) typical R.C.C. slab, (ii) doubly curved earthen slab system (iii) concrete slab with same structural form Table 4-1was calculated as follows. All the rates were calculated from the Building Schedule of Rates (BSR-2019/2020) in Sri Lanka.

4.1 Basis for calculation (small scale to actual scale cost prediction)

The cost was calculated to construct each slab system for a typical room size of 3m x 3m footprint area. For a typical concrete slab system, the thickness was taken as 150mm while reinforcement was taken as hot-rolled reinforcement bars at 150mm in both ways (H-10@150B/W). 1m x 1m size small-scale model was constructed, and the cost was calculated initially. Then the cost for a 3m x 3m earthen slab system is predicted accordingly.

4.2 Cost summary for proposed method

Total labour cost constitutes that for the construction as well as the material preparation: e.g., drying and sieving of the soil. For preparation of Mud-concrete mixture, it requires set of sieves which is not readily available on market. Since the sieves can be used in other mud-concrete practices, cost for the sieves consider as indirect costing and excluded from cost calculation (Table 4-1).

Table 4-1: Cost comparison for three different slab systems

	Traditional R.C.C. Slab system Amount (LKR)	**Doubly curved shell with earthen materials** Amount (LKR)	**Doubly curved shell with concrete** Amount (LKR)
Material Cost			
Filling material	596.86	148.00	638.64
Reinforcement	308.56	-	-
Formwork	281.00	343.50	343.50
Labour cost	191.77	224.79	148.59
Total cost per sq. ft	1378.19	716.29	1130.73
Cost reduction	**0%**	**48%**	**18%**

4.3 Embodied energy calculation for the proposed method

Production and construction stage were considered for embodied energy calculations (Gibbons and Orr, 2020; Udawattha and Halwatura, 2016). According to the work conducted, for a 9 m^2 foot-print area, soil volume of 4.56 m^3 is required and no energy is required for manual excavation of soil. Also, according to the local regulations, 25km of hauling distance was considered for the soil transportation and for the cement transportation it was assumed as 50 km Table 4-2 (Fay and Raniga, 2000; Jayasinghe, 2011).

Table 4-2: Embodied energy calculations for three different slab systems

Traditional R.C.C. Slab system				
Material	Unit	Qty.	Energy per unit in MJ	Embodied Energy in MJ
Reinforced concrete slab	m2	9	730	6570
Formwork material				
Plywood	Kg	70.2	15	1053
Total EE				**7623.00**
Doubly curved shell with earthen materials				
Material	Unit	Qty.	Energy per unit in MJ	Embodied Energy in MJ
Soil (Transport)	m3	4.56	43.75	199.5
Cement	Kg	200	5.85	1170
Transport	Ton.	0.2	50	10
Formwork material				
Plywood	Kg	108.7	15	1630.5
Cement soil sand mortar	m3	1.2	773	927.6
Total EE				**3937.60**
Doubly curved shell with concrete				
Material	Unit	Qty.	Energy per unit in MJ	Embodied Energy in MJ
Concrete 1:2:4	m3	2.4	1664	3993.6
Formwork material				
Plywood	m3	0.167	8520	1422.84
Cement soil sand mortar	m3	1.2	773	927.6
Total EE				**6344.04**

4.4 Summary, findings and conclusions

Material cost was separated into two parts; filling materials and reinforcements. It is clear that the 48% of cost reduction in the earthen slab system is mainly due to the filling materials. Similar trend was also observed in the embodied energy calculations. Further cost reduction can be expected from improving formwork. For the design, plywood formwork with masonry cement mortar was used. However, for modular construction, steel formwork would be ideal as the formwork cost can be spread out among multiple earthen slab systems.

Also, both the structural shell and the ballast loading of the slab system have same density. However, self-weight of the ballast loading can be further reduced by implementing aerated Mud-Concrete mixture or utilizing construction demolition waste into the concrete mixture (This is traditional practise with Catalan thin tile vaulting systems in Spain).

The key findings are summarized below:

- Nearly, 48% of both cost reduction and embodied energy saving could be expected, compared with conventional reinforced slab system having identical footprint areas.
- Labour cost is slightly higher than conventional reinforced concrete slabs due to the labour-intensive soil sieving process. However, such cost can be brought down as novel technologies get widely adopted.

Mud-concrete would be an appropriate construction that can be used to develop compression only slab system.

5 CONCLUSIONS & RECOMANDATIONS

The work presented in the thesis supports the proposal of using an earthen slab system using doubly-curved shell to achieve better economic and environmental performance. The analysis results lead to identify other important aspects of this technique regarding the strength of the slab system. The key findings from the study are concluded as follows.

1. Most of the embodied energy in a typical multi-storey building structure (60% to 70%), exists within the floors. It was identified that; earthen slab system would be huge step towards archiving fully sustainable design.
2. Thin-shell structures were identified as potential structural system for slab systems which results reduction in material usage. However, cost of the modern shell constructions is comparatively high. Thus, mud-concrete was found to be a potential material to developed as slab system by incorporating with shells.
3. Preliminary results indicate that the most suitable thickness for each shell and ballast loading as 50mm thickness from the apex.
4. Peak stresses are concentrated at the mid-span of the slab system for smaller size vaults, since the edge beams and walls act more rigidly for the slab system. However, for larger rectangular or square sections, peak stresses are concentrated at the four edges.
5. Asymmetric live loading is critical for these types of shells. Most prominent asymmetric loading for larger sections were identified when the load is applied over half of the span.
6. A masonry cement mould with framework would be ideal small constructions, to get the correct doubly curved shell shape of the underside of the structure, while for modular constructions a steel formwork would be more suitable.
7. For the construction process, it is ideal to fill the shell component first and then filling the ballast loading to an indicated level. Since the total load of the filling will act as evenly across the formwork.
8. Mud-concrete would be an appropriate construction that can be used to develop compression only slab system.

This is focus on the developing a doubly curved earthen shell slab system. For an eco-friendly and sustainable approach, Mud-concrete was used as construction material instead of typical reinforced concrete. The strength of the slab system comes from its curved shape. For local context, this could be an ideal solution to go for a fully earthen multi-storey construction. Also, due to the low-cost construction practice, this could potentially use to replace the dwelling units in rural areas where material cost is significantly higher.

The following recommendations can be made to build up on the findings presented in this dissertation.

Recommendations for future works;

- Physical model testing should need be carried out for a large-scale model to identify the behavior of the structure under dynamic loading.
- Structural analysis should need to be further explore to identify the seismic resistant of the structure.

Recommendations to engineering practices;

- Possible strategy to identify a satisfactorily close to ideal design for any scale of shell construction should need to be explore. In such way, to estimate the initial span to height ratio for a predefined span of the shell structure.
- Research should need to be conduct to optimize the construction sequence. Especially in the areas to cut down on curing period and formwork/falsework removal time or to cut down labor-intensive sieving process.
- Furthermore, the proposed slab system has interesting visual features as the dome type interior enhance the perception of space. The interior surface texture has a pleasing smooth yellowish brown earthy texture and with a transparent protective coating, interior texture could be retained while improving the durability of the earthen slab system.

REFERENCES

Akadiri, P.O., Chinyio, E.A., Olomolaiye, P.O., 2012. Design of a sustainable building: A conceptual framework for implementing sustainability in the building sector. Buildings 2, 126–152. https://doi.org/10.3390/buildings2020126

Allwood, J.M., Cullen, J.M., Milford, R.L., 2010. Options for achieving a 50% cut in industrial carbon emissions by 2050. Environ. Sci. Technol. 44, 1888–1894. https://doi.org/10.1021/es902909k

Arooz, F.R., Halwatura, R.U., 2018. Mud-concrete block (MCB): mix design & durability characteristics. Case Stud. Constr. Mater. 8, 39–50. https://doi.org/10.1016/j.cscm.2017.12.004

Arooz, R., 2019. In-situ Mud-Concrete as a material for load-bearing walls and sustainable building practices.

Block, P., DeJong, M., Davis, L., Ochsendorf, J., 2010. Tile vaulted systems for low-cost construction in Africa. ATDF J. 7.

Bolay, J.-C., 2020. Convoluted Urban Planning. pp. 83–119. https://doi.org/10.1007/978-3-030-28419-0_4

Chilton, J., Chuang, C.C., 2017. Rooted in Nature: Aesthetics, Geometry and Structure in the Shells of Heinz Isler. Nexus Netw. J. 19, 763–785. https://doi.org/10.1007/s00004-017-0357-5

Dick, G., 2019. Green Building Materials [WWW Document]. URL https://www.calrecycle.ca.gov/greenbuilding/materials (accessed 6.10.21).

EN 1991-1-1: Eurocode 1: Actions on structures - Part 1-1: General actions - Densities, self-weight, imposed loads for buildings, 1991.

Fay, R., Raniga, U.I., 2000. Life-cycle energy analysis of buildings: A case study. Build. Res. Inf. 28, 31–41. https://doi.org/10.1080/096132100369073

Foraboschi, P., Mercanzin, M., Trabucco, D., 2014. Sustainable structural design of tall buildings based on embodied energy. Energy Build. 68, 254–269. https://doi.org/10.1016/j.enbuild.2013.09.003

Froeschle, L.M., 1999. Environmental Assessment and Specification of Green Building Materials. Constr. Specif.

Galabada, H., Halwatura, R.U., 2019. A preliminary study on the use of soil as a floor finishing material, in: 2019 From Innovation to Impact, FITI 2019. Institute of Electrical and Electronics Engineers Inc. https://doi.org/10.1109/FITI49428.2019.9037635

Gibbons, O.P., Orr, J.J., 2020. How to calculate Embodied Carbon.

Guggemos, A.A., Horvath, A., 2006. Decision-Support Tool for Assessing the Environmental Effects of Constructing Commercial Buildings. J. Archit. Eng. 12, 187–195. https://doi.org/10.1061/(asce)1076-0431(2006)12:4(187)

Hammond, G.P., Jones, C.I., 2008. Embodied energy and carbon in construction materials. Proc. Inst. Civ. Eng. Energy 161, 87–98. https://doi.org/10.1680/ener.2008.161.2.87

Hawkins, W., 2019. Thin-shell concrete floors for sustainable buildings. Dr. Thesis.

IEA, 2008. Energy Technology Perspectives 2018: Scenarios & Strategies to 2050 [WWW Document]. URL https://www.iea.org/topics/energy-technology-perspectives (accessed 7.4.21).

IS 6332 (1984): Code of practice for construction of floor and roofs using precast doubly-curved shell units, 2000.

Jayasinghe, C., 2011. Embodied energy of alternative building materials and their impact on life cycle cost parameters. Int. Conf. Struct. Eng. Constr. Manag. December 16-18, 2011, Kandy, Sri Lanka 1–20. https://doi.org/10.13140/RG.2.1.4852.2321

Jayasinghe, R.R., Nanayakkara, K.I.., Arooz, F.R., Halwatura, R.U., 2019. Catalan Vault Inspired Earthen Slab System for Houses in Sri Lanka: Form-Finding.

Leung, N., 2018. The Nature of Gridshell Form Finding – WeWantToLearn.net [WWW Document]. URL https://wewanttolearn.wordpress.com/2018/03/13/the-nature-of-gridshell-form-finding/ (accessed 9.18.21).

López, D., Domènech Rodríguez, M., Palumbo Fernández, M., 2014. “Brick-topia”, the thin-tile vaulted pavilion. Case Stud. Struct. Eng. 2, 33–40. https://doi.org/10.1016/j.csse.2014.09.001

Mansoori, M., Kalantar, N., Creasy, T., Rybkowski, Z., 2019. Adaptive wooden architecture. designing a wood composite with shape-memory behavior, in: Digital Wood Design. Springer, pp. 703–717. https://doi.org/10.1007/978-3-030-03676-8_27

Menegaki, M., Damigos, D., 2018. A review on current situation and challenges of construction and demolition waste management. Curr. Opin. Green Sustain. Chem. 13, 8–15. https://doi.org/10.1016/J.COGSC.2018.02.010

Menne, M.J., Williams, C.N., Gleason, B.E., Jared Rennie, J., Lawrimore, J.H., 2018. The Global Historical Climatology Network Monthly Temperature Dataset, Version 4. J. Clim. 31, 9835–9854. https://doi.org/10.1175/JCLI-D-18-0094.1

Michiels, T., Adriaenssens, S., 2017. Identification of key design parameters for earthquake resistance of reinforced concrete shell structures. Eng. Struct. 153, 411–420. https://doi.org/10.1016/j.engstruct.2017.10.043

Moriana, R.G., 2012. Gaudí’s hanging chain models: parametric design avant la lettre? – Criticalista [WWW Document]. URL https://criticalista.com/2012/08/16/gaudis-hanging-chain-models-parametric-design-avant-la-lettre/ (accessed 6.10.21).

Ockleston, A.J., 1958. Loading tests on reinforced concrete slabs spanning in two directions. Portland Cement Institute.

Oval, R., Rippmann, M., Mele, T. Van, Baverel, O., Oval, R., Rippmann, M., Mele, T. Van, Baverel, O., Block, P., 2018. Patterns for Masonry Vault Design To cite this version : HAL Id : hal-01883502.

Patnaik, R., 2018. Impact of Industrialization on Environment and Sustainable Solutions - Reflections from a South Indian Region, in: IOP Conference Series: Earth and Environmental Science. Institute of Physics Publishing, p. 12016. https://doi.org/10.1088/1755-1315/120/1/012016

Pollock, S., 1999. Ancient Mesopotamia [WWW Document]. URL https://books.google.lk/books/about/Ancient_Mesopotamia.html?id=ndjc_5xhlDsC&redir_esc=y (accessed 6.10.21).

Preston, F., Lehne, J., 2018. Making Concrete Change Innovation in Low-carbon Cement and Concrete. Environ. Sci.

Rajabzadeh, S., Sassone, M., 2013. Reviving the Design of Contemporary Masonry Vaults, in: ATINER'S Conference.

Rippmann, M., Block, P., 2012. rhino VAULT 1–12.

Sustainable Development Goals (SDGs) and Disability [WWW Document], 2020. URL https://www.un.org/development/desa/disabilities/about-us/sustainable-development-goals-sdgs-and-disability.html (accessed 6.10.21).

Udawattha, C. and, Halwatura, R., 2016. The embodied energy and life cycle costing: A case study on basic dwellings in Sri Lanka. Natl. Green Conf. 2016 Univ. Kelaniya 18, 1–10.

Udawattha, C., Galabada, H., Halwatura, R., 2017. Mud concrete paving block for pedestrian pavements. Case Stud. Constr. Mater. 7, 249–262. https://doi.org/10.1016/j.cscm.2017.08.005

Walker, P., Keable, R., Martin, J., Maniatidis, V., 2005. Rammed earth: design and construction guidelines. Watford: BRE.

APPENDIX A

Analysis for 1m x 1m slab system

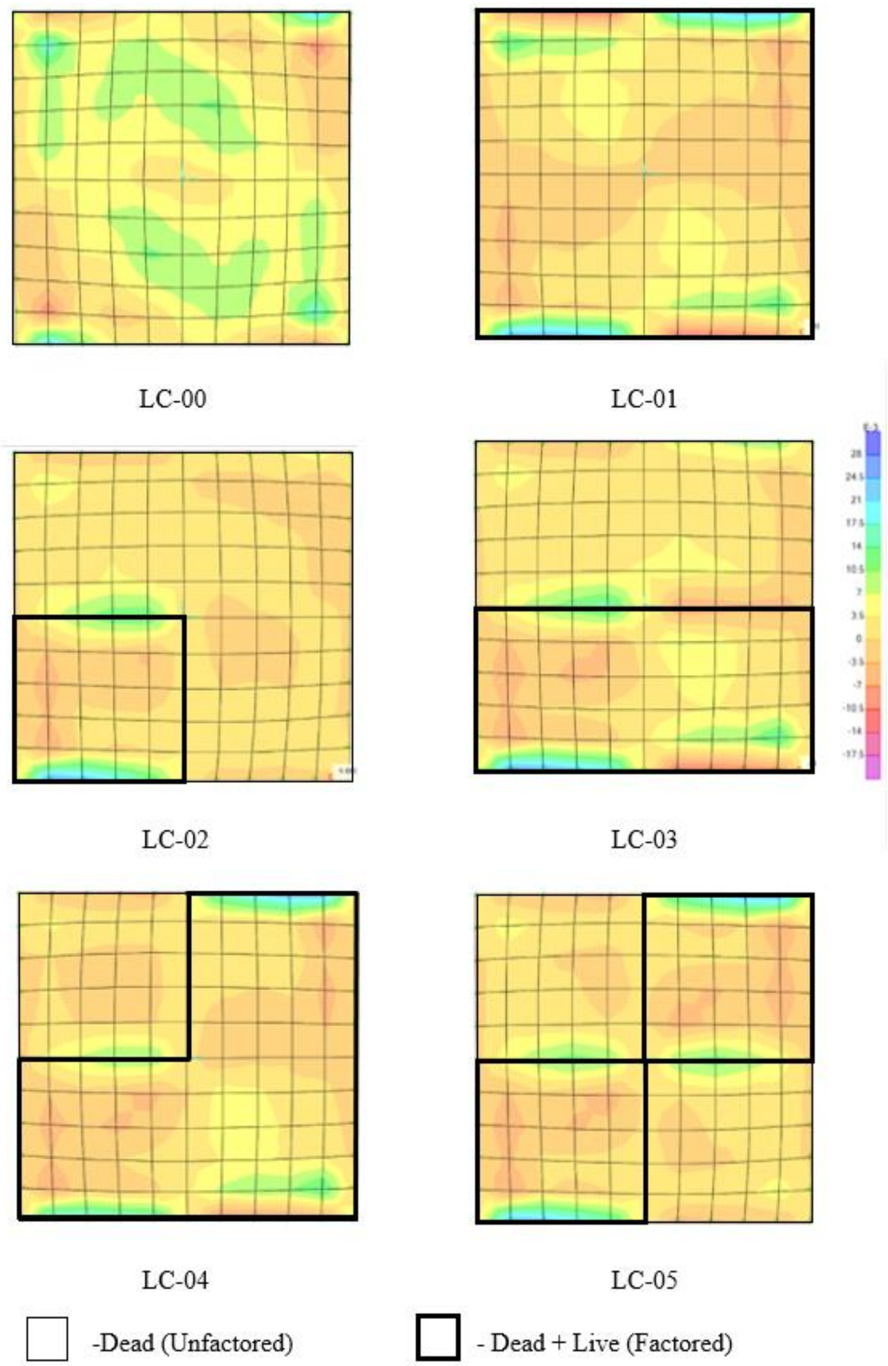

Stress distribution across the 1m x 1m shell at the design loading for each live loading patterns while live load of 2kN/m^2 outlined in bold

Load case analysis for 1m x 1m shell with ballast loading

Load Case	Maximum tensile stress	Maximum Compressive stress
	N/mm^2	N/mm^2
LC-00	0.0031	0.0053
LC-01	0.0140	0.0240
LC-02	0.0120	0.0200
LC-03	0.0130	0.0210
LC-04	0.0140	0.0240
LC-05	0.0130	0.0200

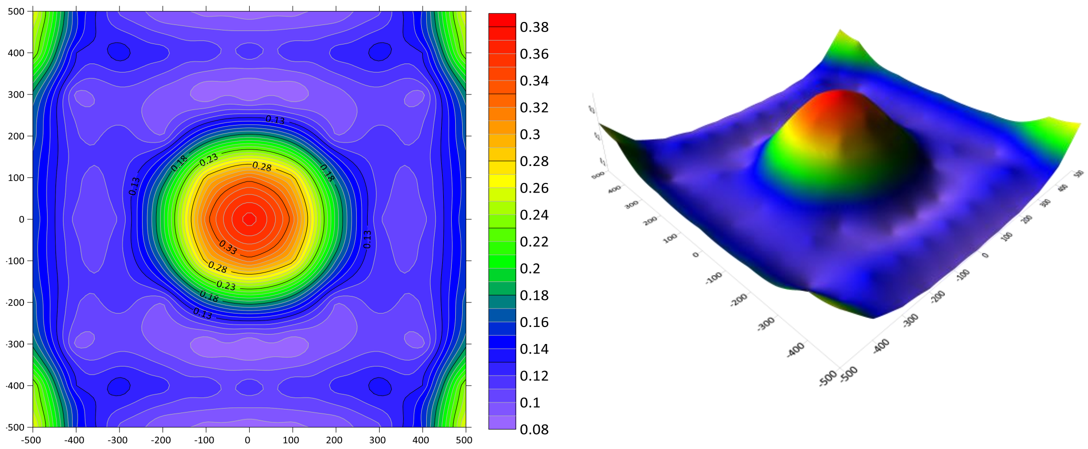

Tensile stress distribution of 1m x 1m vault, when the concentrated point load of 2kN acting on each grid point (Illustrated with Surfer16)

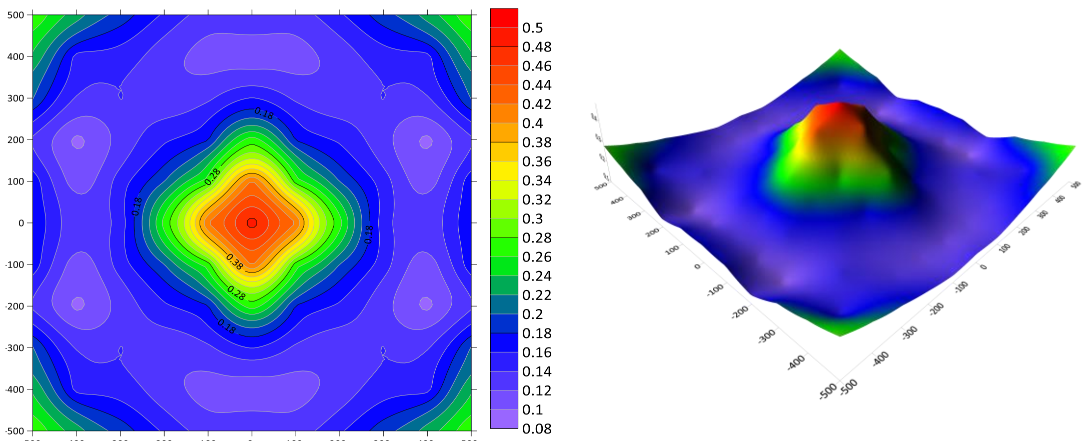

Compressive stress distribution of 1m x 1m vault, when the concentrated point load of 2kN acting on each grid point (Illustrated with Surfer16)

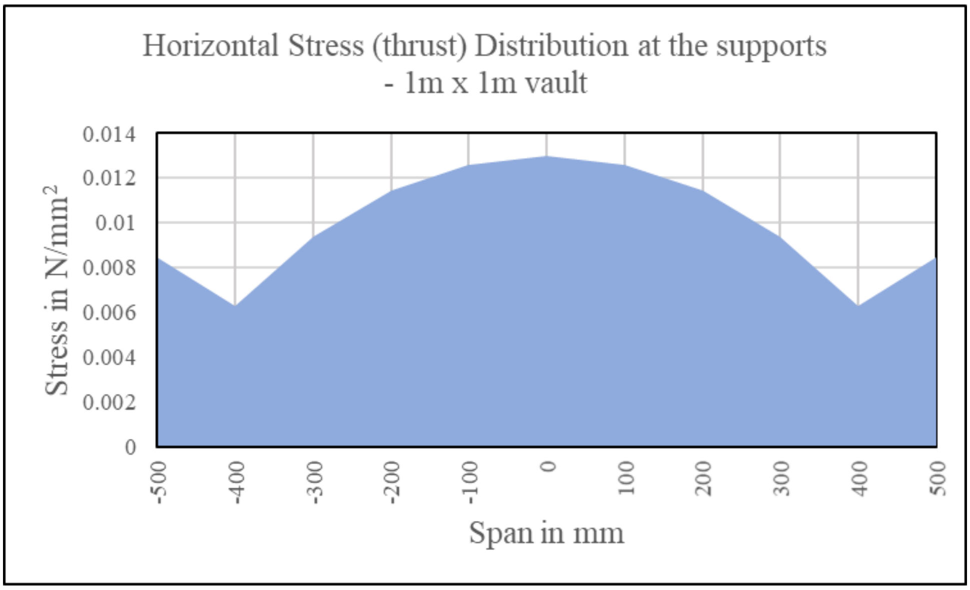

Horizontal stress (thrust) distribution of 1m x 1m vault at the supports

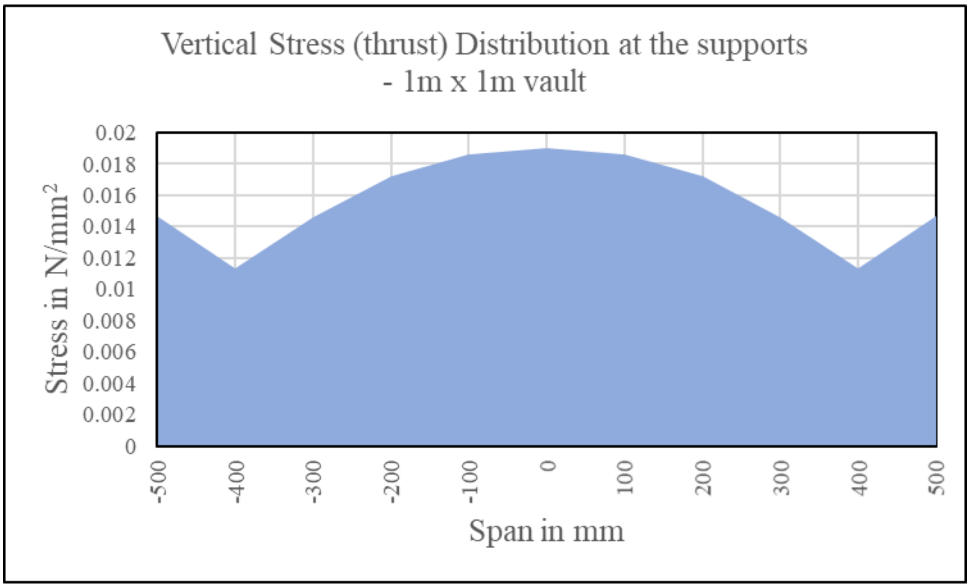

Vertical stress (thrust) distribution of 1m x1m vault at the supports

APPENDIX B

Sieve analysis for three different soil samples to identify the most suitable soil sample for Mud-concrete construction

Soil Sample I							
Sieve Size	Mass of Empty Sieve	Mass of Sieve + Soil Retained	Soil Retained	Percentage by Weight	Cumulative Passing	Percent Retained	Percent Passing
mm	g	g	g	%	g	%	%
32.000	578.700	580.520	1.8	0.10	1830.1	0.10	99.90
19.000	576.10	608.60	32.5	1.77	1797.6	1.87	98.13
4.750	87.70	879.40	791.7	43.22	1005.9	45.09	54.91
0.425	87.60	934.20	846.6	46.21	159.3	91.30	8.70
0.000	365.30	524.60	159.3	8.70	0.0	100.00	0.00
Total Weight			1831.92	100.0			

Sample II							
Sieve Size	Mass of Empty Sieve	Mass of Sieve + Soil Retained	Soil Retained	Percentage by Weight	Cumulative Passing	Percent Retained	Percent Passing
mm	g	g	g	%	g	%	%
32.000	578.700	583.540	4.8	0.45	1080.1	0.45	99.55
19.000	576.10	706.40	130.3	12.01	949.8	12.46	87.54
4.750	569.90	1135.60	565.7	52.14	384.1	64.60	35.40
0.425	452.90	767.80	314.9	29.02	69.2	93.62	6.38
0.000	365.30	434.50	69.2	6.38	0.0	100.00	0.00
Total Weight			1084.94	100.0			

Sample III							
Sieve Size	Mass of Empty Sieve	Mass of Sieve + Soil Retained	Soil Retained	Percentage by Weight	Cumulative Passing	Percent Retained	Percent Passing
mm	g	g	g	%	g	%	%
32.000	578.700	578.700	0.0	0.00	742.4	0.00	100.00
19.000	576.10	620.40	44.3	5.97	698.1	5.97	94.03
4.750	569.90	891.00	321.1	43.25	377.0	49.22	50.78
0.425	452.90	773.40	320.5	43.17	56.5	92.39	7.61
0.000	365.30	421.80	56.5	7.61	0.0	100.00	0.00
Total Weight			742.40	100.0			

APPENDIX C

Structural analysis data

Compressive stresses for various shell thicknesses

Compressive stresses of the shell for various shell thicknesses															
Code	Vault dimensions in mm	Shell thickness in mm	Rise in mm	**S11 Top**	**S22 Top**	**S12 Top**	**Smax Top**	**Smin Top**	**S11 Bot**	**S22 Bot**	**S12 Bot**	**Smax Bot**	**Smin Bot**	**SVM Bot**
				N/mm^2	N/mm^2	N/mm^2	N/mm^2	N/mm^2	N/mm^2	N/mm^2	N/mm^2	N/mm^2	N/mm^2	N/mm^2
A-ST-1	1000 x 1000	25	100	0.255	0.254	0.137	0.259	0.083	0.261	0.258	0.135	0.267	0.093	0.385
A-ST-2	1000 x 1000	50	100	0.122	0.153	0.068	0.154	0.043	0.124	0.153	0.067	0.154	0.043	0.189
A-ST-3	1000 x 1000	75	100	0.071	0.098	0.04	0.098	0.027	0.073	0.098	0.039	0.098	0.028	0.114
A-ST-4	1000 x 1000	100	100	0.048	0.071	0.027	0.071	0.019	0.049	0.07	0.026	0.07	0.019	0.078
B-ST-1	3000 x 3000	25	300	0.615	0.914	0.272	0.914	0.315	0.558	0.908	0.279	0.908	0.247	0.822
B-ST-2	3000 x 3000	50	300	0.166	0.272	0.077	0.272	0.073	0.151	0.271	0.078	0.271	0.072	0.244
B-ST-3	3000 x 3000	75	300	0.051	0.087	0.024	0.087	0.023	0.046	0.087	0.024	0.087	0.023	0.078
B-ST-4	3000 x 3000	100	300	0.012	0.021	0.0057	0.021	0.00566	0.011	0.021	0.00572	0.021	0.00557	0.019
C-ST-1	6000 x 3000	25	600	0.544	0.661	0.23	0.661	0.316	0.528	0.652	0.245	0.653	0.22	0.596
C-ST-2	6000 x 3000	50	600	0.158	0.238	0.074	0.238	0.076	0.148	0.236	0.074	0.236	0.065	0.213
C-ST-3	6000 x 3000	75	600	0.05	0.085	0.024	0.085	0.024	0.047	0.084	0.024	0.084	0.023	0.076
C-ST-4	6000 x 3000	100	600	0.012	0.022	0.00593	0.022	0.00619	0.011	0.022	0.00569	0.022	0.00607	0.02

Tensile stresses for various shell thicknesses

Tensile stresses of the shell for various shell thicknesses															
Code	Vault dimensions in mm	Shell thickness in mm	Rise in mm	**S11 Top**	**S22 Top**	**S12 Top**	**Smax Top**	**Smin Top**	**S11 Bot**	**S22 Bot**	**S12 Bot**	**Smax Bot**	**Smin Bot**	**SVM Bot**
				N/mm^2	N/mm2	N/mm2	N/mm2	N/mm2	N/mm2	N/mm2	N/mm2	N/mm2	N/mm2	N/mm2
A-ST-1	1000 x 1000	25	100	-0.318	-0.432	-0.105	-0.168	-0.432	-0.302	-0.421	-0.118	-0.121	-0.422	0.02
A-ST-2	1000 x 1000	50	100	-0.138	-0.212	-0.053	-0.063	-0.212	-0.133	-0.21	-0.055	-0.057	-0.21	0.011
A-ST-3	1000 x 1000	75	100	-0.078	-0.127	-0.033	-0.036	-0.127	-0.075	-0.127	-0.035	-0.034	-0.127	0.00727
A-ST-4	1000 x 1000	100	100	-0.051	-0.087	-0.023	-0.025	-0.087	-0.05	-0.087	-0.024	-0.023	-0.087	0.00512
B-ST-1	3000 x 3000	25	300	-0.444	-0.633	-0.288	-0.177	-0.633	-0.499	-0.634	-0.299	-0.192	-0.634	0.06
B-ST-2	3000 x 3000	50	300	-0.128	-0.211	-0.08	-0.056	-0.211	-0.146	-0.211	-0.082	-0.057	-0.211	0.0042
B-ST-3	3000 x 3000	75	300	-0.042	-0.071	-0.025	-0.019	-0.071	-0.046	-0.071	-0.026	-0.019	-0.071	0.00073
B-ST-4	3000 x 3000	100	300	-0.01	-0.018	-0.006	-0.0047	-0.018	-0.011	-0.018	-0.0061	-0.0047	-0.018	0.00019
C-ST-1	6000 x 3000	25	600	-0.352	-0.435	-0.23	-0.124	-0.436	-0.37	-0.439	-0.246	-0.166	-0.439	0.018
C-ST-2	6000 x 3000	50	600	-0.116	-0.172	-0.076	-0.047	-0.172	-0.132	-0.172	-0.078	-0.051	-0.172	0.00124
C-ST-3	6000 x 3000	75	600	-0.04	-0.064	-0.026	-0.017	-0.064	-0.044	-0.063	-0.025	-0.017	-0.063	0.00197
C-ST-4	6000 x 3000	100	600	-0.01	-0.017	-0.0063	-0.0045	-0.017	-0.011	-0.017	-0.006	-0.0045	-0.017	0.00033

Load case analysis for 1mx1m shell

Load Case	Compressive Stresses of the shell - 2kN/m2 acting on the 1mx1m shell with ballast loading															
	S11 Top	S22 Top	S12 Top	Smax Top	Smin Top	SVM Top	S11 Bot	S22 Bot	S12 Bot	Smax Bot	Smin Bot	SAngle Bot	SVM Bot	S13 Avg	S23 Avg	Smax Avg
	N/mm^2	N/mm^2	N/mm^2	N/mm^2	N/mm^2	N/mm^2	N/mm^2	N/mm^2	N/mm^2	N/mm^2	N/mm^2	N/mm^2	N/mm^2	N/mm^2	N/mm^2	N/mm^2
LC-00	0.0029	0.0052	0.0014	0.0053	0.0028	0.0048	0.0029	0.0052	0.0014	0.0053	0.0028	89.8080	0.0048	0.0004	0.0008	0.0008
LC-01	0.0084	0.0230	0.0046	0.0240	0.0082	0.0360	0.0084	0.0230	0.0046	0.0240	0.0082	89.8330	0.0360	0.0016	0.0045	0.0045
LC-02	0.0097	0.0210	0.0041	0.0210	0.0088	0.0250	0.0100	0.0200	0.0040	0.0200	0.0060	89.9690	0.0250	0.0012	0.0037	0.0038
LC-03	0.0100	0.0200	0.0056	0.0210	0.0076	0.0280	0.0100	0.0200	0.0056	0.0210	0.0076	89.9870	0.0280	0.0020	0.0037	0.0037
LC-04	0.0096	0.0240	0.0049	0.0240	0.0094	0.0330	0.0090	0.0240	0.0057	0.0240	0.0087	89.9680	0.0330	0.0016	0.0045	0.0045
LC-05	0.0089	0.0200	0.0034	0.0210	0.0082	0.0260	0.0093	0.0200	0.0038	0.0200	0.0062	89.9880	0.0260	0.0012	0.0037	0.0038

Load Case	Tensile Stresses of the shell - 2kN/m2 acting on the quadrant of 1mx1m shell with ballast loading															
	S11 Top	S22 Top	S12 Top	Smax Top	Smin Top	SVM Top	S11 Bot	S22 Bot	S12 Bot	Smax Bot	Smin Bot	SAngle Bot	SVM Bot	S13 Avg	S23 Avg	Smax Avg
	N/mm^2	N/mm^2	N/mm^2	N/mm^2	N/mm^2	N/mm^2	N/mm^2	N/mm^2	N/mm^2	N/mm^2	N/mm^2	N/mm^2	N/mm^2	N/mm^2	N/mm^2	N/mm^2
LC-00	-0.003	-0.006	-0.0012	-0.00309	-0.0056	6.7E-05	-0.0032	-0.0056	-0.0012	-0.0031	-0.0056	-89.787	6.7E-05	-0.0004	-8E-04	4.6E-05
LC-01	-0.015	-0.04	-0.0053	-0.014	-0.04	0.00099	-0.015	-0.04	-0.0053	-0.014	-0.04	-89.005	0.00099	-0.0016	-0.005	0.00017
LC-02	-0.011	-0.028	-0.0034	-0.00799	-0.028	0.00031	-0.012	-0.027	-0.004	-0.012	-0.027	-89.462	0.00012	-0.0016	-0.002	2.1E-06
LC-03	-0.013	-0.031	-0.005	-0.013	-0.031	0.00073	-0.013	-0.031	-0.005	-0.013	-0.031	-89.988	0.00073	-0.002	-0.004	5E-05
LC-04	-0.014	-0.037	-0.0062	-0.014	-0.037	0.00063	-0.014	-0.037	-0.0055	-0.014	-0.037	-89.506	0.0008	-0.0017	-0.004	4E-05
LC-05	-0.01	-0.029	-0.0031	-0.00826	-0.029	0.00091	-0.013	-0.029	-0.0031	-0.013	-0.029	-89.967	0.00088	-0.0016	-0.004	4.6E-05

Load case analysis for 3mx3m shell

Load Case	Compressive Stresses of the shell - 2kN/m2 acting on the quadrant of 3mx3m shell with ballast loading															
	S11 Top	S22 Top	S12 Top	Smax Top	Smin Top	SVM Top	S11 Bot	S22 Bot	S12 Bot	Smax Bot	Smin Bot	SAngle Bot	SVM Bot	S13 Avg	S23 Avg	Smax Avg
	N/mm^2	N/mm^2	N/mm^2	N/mm^2	N/mm^2	N/mm^2	N/mm^2	N/mm^2	N/mm^2	N/mm^2	N/mm^2	N/mm^2	N/mm^2	N/mm^2	N/mm^2	N/mm^2
LC-00	0.044	0.153	0.015	0.153	0.044	0.197	0.044	0.153	0.015	0.153	0.044	89.955	0.197	0.0048	0.029	0.029
LC-01	0.049	0.179	0.017	0.179	0.048	0.241	0.049	0.179	0.017	0.179	0.048	89.894	0.241	0.0053	0.035	0.035
LC-02	0.063	0.232	0.022	0.232	0.063	0.304	0.064	0.232	0.022	0.232	0.064	89.954	0.304	0.0069	0.028	0.045
LC-03	0.063	0.231	0.021	0.231	0.063	0.316	0.063	0.231	0.021	0.231	0.063	89.997	0.316	0.0093	0.046	0.046
LC-04	0.063	0.231	0.02	0.231	0.063	0.311	0.063	0.231	0.021	0.231	0.063	89.998	0.311	0.0068	0.037	0.045
LC-05	0.043	0.16	0.015	0.16	0.043	0.209	0.045	0.16	0.015	0.16	0.044	89.992	0.209	0.0049	0.022	0.031

Load Case	Tensile Stresses of the shell - 2kN/m2 acting on the quadrant of 3mx3m shell with ballast loading															
	S11 Top	S22 Top	S12 Top	Smax Top	Smin Top	SVM Top	S11 Bot	S22 Bot	S12 Bot	Smax Bot	Smin Bot	SAngle Bot	SVM Bot	S13 Avg	S23 Avg	Smax Avg
	N/mm^2	N/mm^2	N/mm^2	N/mm^2	N/mm^2	N/mm^2	N/mm^2	N/mm^2	N/mm^2	N/mm^2	N/mm^2	N/mm^2	N/mm^2	N/mm^2	N/mm^2	N/mm^2
LC-00	-0.059	-0.219	-0.017	-0.059	-0.219	0.00052	-0.059	-0.219	-0.017	-0.059	-0.219	-90	0.00052	-0.0048	-0.029	0.0001
LC-01	-0.072	-0.269	-0.018	-0.072	-0.269	0.00062	-0.072	-0.269	-0.018	-0.072	-0.269	-89.978	0.00062	-0.0053	-0.035	0.00019
LC-02	-0.087	-0.338	-0.024	-0.087	-0.338	0.00055	-0.091	-0.337	-0.021	-0.091	-0.337	-89.999	0.00067	-0.0084	-0.045	1.5E-05
LC-03	-0.094	-0.352	-0.027	-0.094	-0.352	0.00167	-0.094	-0.352	-0.027	-0.094	-0.352	-89.997	0.00167	-0.0093	-0.046	5.6E-05
LC-04	-0.09	-0.346	-0.024	-0.09	-0.346	0.00046	-0.093	-0.345	-0.022	-0.093	-0.345	-89.982	0.0008	-0.0084	-0.045	1.8E-05
LC-05	-0.06	-0.232	-0.017	-0.06	-0.232	0.00128	-0.062	-0.232	-0.015	-0.062	-0.232	-89.981	0.00147	-0.0042	-0.031	1.4E-05

Load case analysis for 6mx3m shell

Load Case	**Compressive Stresses of the shell - 2kN/m2 acting on the quadrant of 6mx3m shell with ballast loading**															
	S11 Top	S22 Top	S12 Top	Smax Top	Smin Top	SVM Top	S11 Bot	S22 Bot	S12 Bot	Smax Bot	Smin Bot	SAngle Bot	SVM Bot	S13 Avg	S23 Avg	Smax Avg
	N/mm^2	N/mm^2	N/mm^2	N/mm^2	N/mm^2	N/mm^2	N/mm^2	N/mm^2	N/mm^2	N/mm^2	N/mm^2	N/mm^2	N/mm^2	N/mm^2	N/mm^2	N/mm^2
LC-00	0.075	0.192	0.036	0.192	0.055	0.214	0.075	0.192	0.036	0.192	0.055	89.996	0.214	0.021	0.068	0.068
LC-01	0.097	0.256	0.046	0.256	0.07	0.292	0.097	0.256	0.046	0.256	0.07	89.999	0.292	0.027	0.091	0.091
LC-02	0.079	0.24	0.039	0.24	0.064	0.272	0.093	0.239	0.045	0.239	0.068	89.99	0.272	0.026	0.073	0.085
LC-03	0.096	0.256	0.046	0.256	0.07	0.293	0.096	0.256	0.046	0.256	0.07	89.998	0.293	0.027	0.091	0.091
LC-04	0.097	0.256	0.046	0.256	0.07	0.293	0.096	0.256	0.046	0.256	0.07	89.985	0.292	0.027	0.091	0.091
LC-05	0.079	0.24	0.038	0.24	0.064	0.272	0.093	0.239	0.045	0.239	0.068	89.967	0.272	0.026	0.073	0.085

Load Case	**Tensile Stresses of the shell - 2kN/m2 acting on the quadrant of 6mx3m shell with ballast loading**															
	S11 Top	S22 Top	S12 Top	Smax Top	Smin Top	SVM Top	S11 Bot	S22 Bot	S12 Bot	Smax Bot	Smin Bot	SAngle Bot	SVM Bot	S13 Avg	S23 Avg	Smax Avg
	N/mm^2	N/mm^2	N/mm^2	N/mm^2	N/mm^2	N/mm^2	N/mm^2	N/mm^2	N/mm^2	N/mm^2	N/mm^2	N/mm^2	N/mm^2	N/mm^2	N/mm^2	N/mm^2
LC-00	-0.078	-0.238	-0.036	-0.063	-0.238	0.00161	-0.078	-0.238	-0.036	-0.063	-0.238	-89.99	0.00161	-0.021	-0.068	0.00028
LC-01	-0.101	-0.326	-0.047	-0.087	-0.326	0.0029	-0.101	-0.326	-0.047	-0.087	-0.326	-89.994	0.0029	-0.027	-0.091	0.00069
LC-02	-0.097	-0.303	-0.045	-0.08	-0.303	0.0017	-0.082	-0.303	-0.039	-0.081	-0.303	-89.991	0.00044	-0.022	-0.085	1.3E-05
LC-03	-0.101	-0.326	-0.047	-0.087	-0.326	0.00108	-0.101	-0.326	-0.047	-0.087	-0.326	-89.999	0.00108	-0.027	-0.091	0.00033
LC-04	-0.101	-0.326	-0.047	-0.087	-0.326	0.00177	-0.101	-0.326	-0.047	-0.087	-0.326	-89.997	0.00047	-0.027	-0.091	1.3E-05
LC-05	-0.097	-0.302	-0.045	-0.08	-0.302	0.00174	-0.082	-0.303	-0.039	-0.081	-0.303	-89.987	0.00045	-0.023	-0.085	1.3E-05